Thermoplastic Space Point Design (TSPD) Tall Tower Lunar Thermal Analysis

Will Grier, Amanda Stark, Rachel Wiggins, Ruth Amundsen

NASA Langley Research Center
Structural and Thermal Systems Branch (STSB) - D206

Presented By

Will Grier

Thermal & Fluids Analysis Workshop
TFAWS 2024
August 26-30, 2024
NASA Glenn Research Center
Cleveland, OH

Outline

- Study Purpose
- Model Overview
  - Assumptions
- Tower Elements and Properties
- Lunar Surface Environment
- Results
  - Temperatures and Timeline
  - Structural-Thermal Deformation
  - Sensitivity Analyses
- Remarks
  - Findings
  - Future Work
- References

Thermoplastics Development for Exploration Applications (TDEA) Project

- **Project Goal:** Advance NASA's thermoplastic composites capabilities by developing structurally efficient joining solutions for large-scale space structures and applications to support NASA's future exploration missions[1]
- **Project Objective #4:** Develop and understand advanced thermoplastic joining technique(s) relevant to space environments and applicable to unitized and/or reconfigurable composite structures
  - Project developed a point design based on the Tall Lunar Tower (TLT) concept to inform development of in-space assembled thermoplastic composite structures. TLT is robotically assembled and erected on lunar surface to capture solar illumination for power generation.[2]
- **Task:** Identify temperature extremes, gradients, and timelines for a 50-meter-tall thermoplastic composite tower through one year on the south pole of the lunar surface (Shackleton Connecting Ridge)

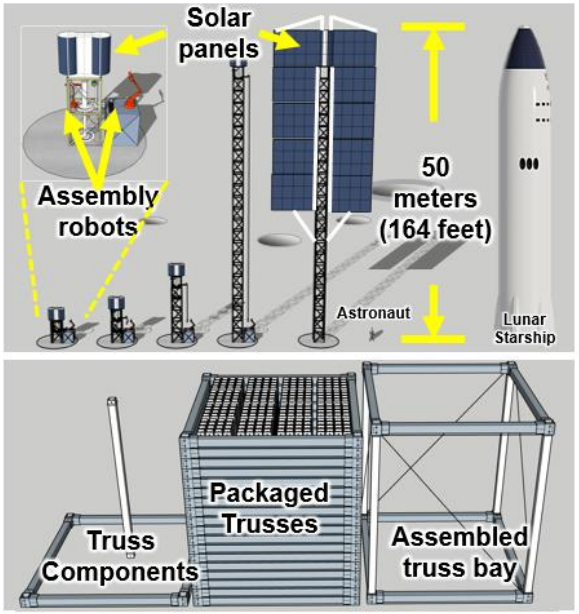

Tall Lunar Tower Concept[2]

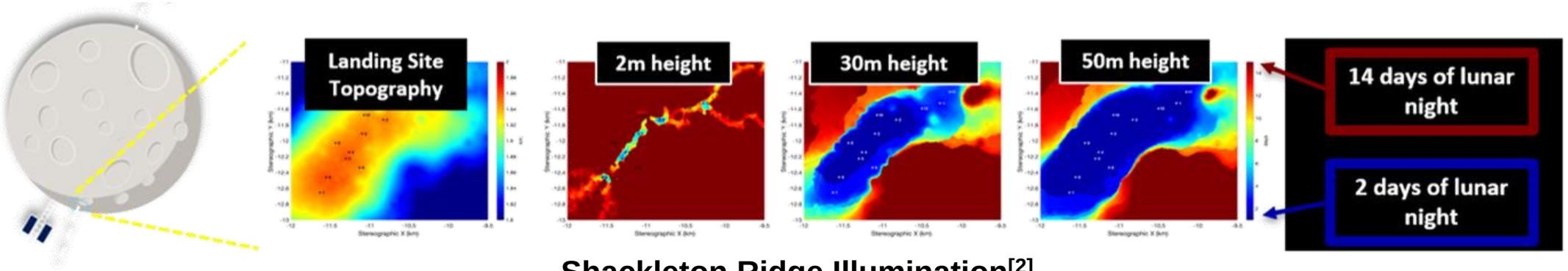

Shackleton Ridge Illumination[2]

Study Purpose

- The surface of the Lunar south pole represents a challenging thermal environment for any space or surface-based asset
- Investigate the viability of using thermoplastic composite materials to construct a tall tower at the Lunar south pole

Task Objectives:

- Compare estimated maximum and minimum temperature values to composite material limits
- Estimate number of days per year the tower base joints remain equivalent to or greater than a specified temperature to inform welding operations
- Investigate sensitivity of results to composite material properties, lunar surface properties, and local terrain

Task Product:

- Thermal modeling and analysis process for assessment of **tall lunar asset operations** at the south pole where illumination conditions are highly dependent on local terrain. Applicable to tall structures including towers, landers, and habitats (e.g., Vertical Solar Array Technology, Human Landing System)

Model Overview

- Lunar environments defined from Design Specification for Natural Environments (DSNE) and analysis methods derived from HLS Lunar Thermal Analysis Guidebook (LTAG)[3,4]
- Lunar Reconasaince Orbiter (LRO) databases[5-8]
  - Diviner Lunar Radiometer Experiment (DLRE), Lunar Orbiter Laser Altimeter (LOLA), and QuickMap Viewer
- Analyzed Shackleton Connecting Ridge (-89.46752, -138.012788 with elevation of 1937.83 meters)
  - 14,630 node surface mesh used to simulate terrain dependent incident solar illumination patterns at south pole
- Thermoplastic Space Point Design (TSPD) tower design
  - 14,200 node tower composed of TC1225/T700 thermoplastic fiber reinforced composite laminate

- Assumptions
  - Tower is fully assembled (incremental build and weld configurations not assessed)
  - Tower is conductively isolated from lunar surface (2 meter separation distance representing lander height)
  - Tower is exposed to thermal radiation environments (no solar panels, robotics, surface treatments, or enclosures)
  - Tower is not covered by lunar regolith (dust impacts not assessed)

Versions: Thermal Desktop = 6.3 Patch 15, TDEA Model = TDEA_v3d_WJG

TSPD Tower Elements

- Simplified CAD geometry for Thermal Desktop
  - Version: TDEA-404, TSPD, RUC ASSEMBLY_20240318
- 51-meter-tall tower with 18 Repeating Unit Cells (RUC)
  - TC1225/T700 fiber reinforced composite laminate
  - Joint welds represented by merged nodes
  - RUCs composed of four structural members
    - Diagonal (TDEA-401, TSPD TRUSS MEMBER, DIAGONAL 20240308)
    - Horizontal (TDEA-402, TSPD TRUSS MEMBER, HORIZONTAL 20240308)
    - Vertical (TDEA-403, TSPD TRUSS MEMBER, VERTICAL 20240308)
    - Joint (TDEA-400, TSPD JOINT SPICE PLATE 20240308)

CAD **Thermal Desktop**

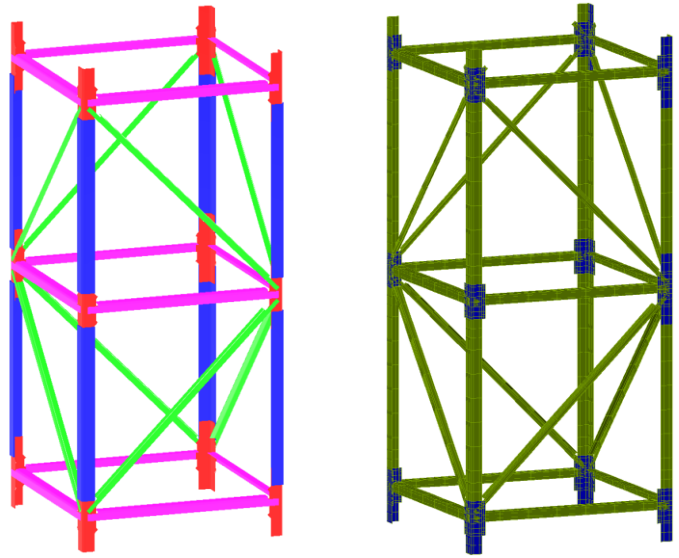

Repeating Unit Cell (RUC)

Tower

CAD

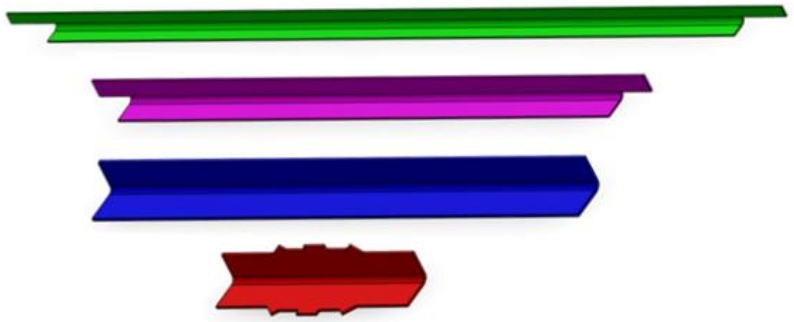

Diagonal Element

Horizontal Element

Vertical Element

Joint Element

Thermal Desktop

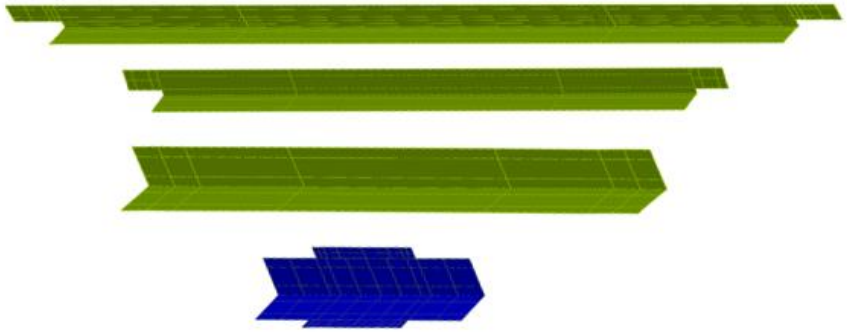

Composite Material Properties

- Multi-directional composite laminate layups and effective thermal conductivity were input into Thermal Desktop model. No material data avilable below 0ºC (polynomial fit)

Material: TC1225/T700 (Fiber Reinforced)		
Property	**Value**	**Source**
Density, ρ [kg/m^3]	1590	Data Sheet[9]
IR Emissivity, ε	0.832	Sample Measurement
Solar Absorptivity, α	0.892	Sample Measurement
Thermal Cond., *k* [W/m/C]	ANISO & Temp Dependent	Test Results
Specific Heat, *c* [J/kg/C]	Temp Dependent	Literature[10]

Composite Laminate Layup Properties:						
Member	**Layup**	**Layers**	**Layup Thickness**	**0°%**	**±45°%**	**90°%**
Diagonal	$[(45,0_2,-45,0_2)_2/0_3]_s$	30	4.11-mm	73.3	13.3	0
Horizontal	$[(45,0_2,-45,0_4)_2/0_3]_s$	38	5.21-mm	78.9	10.5	0
Joint	$[45,90,-45,0_{13},45,90_2,-45,0_6]_s$	52	7.13-mm	73.1	7.7	11.5
Vertical	$[(45,0_3,-45,0_2)_4/0_2]_s$	60	8.23-mm	73.3	13.3	0

Specific Heat

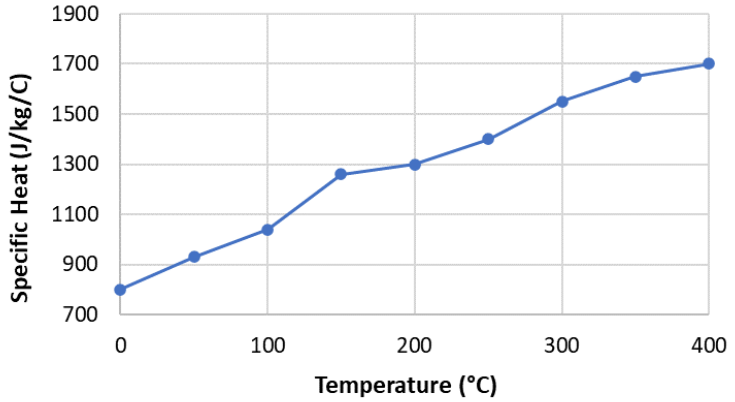

Thermal Conductivity*

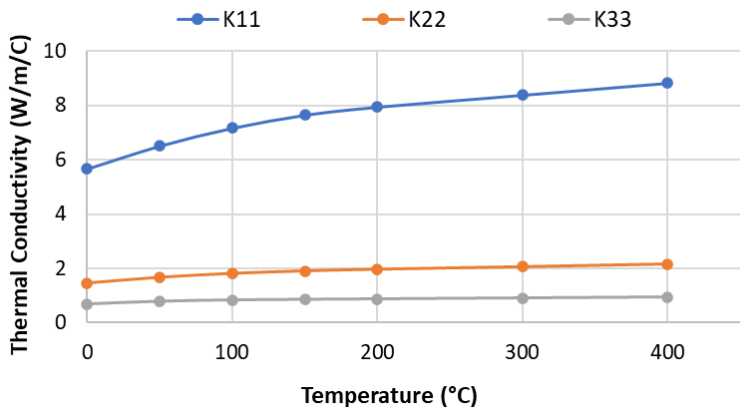

***Note:** Diagonal member thermal conductivity plot shown, other three member plots are similar

Tower Location

- Shackleton Connecting Ridge (-89.46752º, -138.012788º with elevation of 1937.83 meters)
- Specific coordinates chosen to match available average seasonal surface temperature flight data from LRO[6]

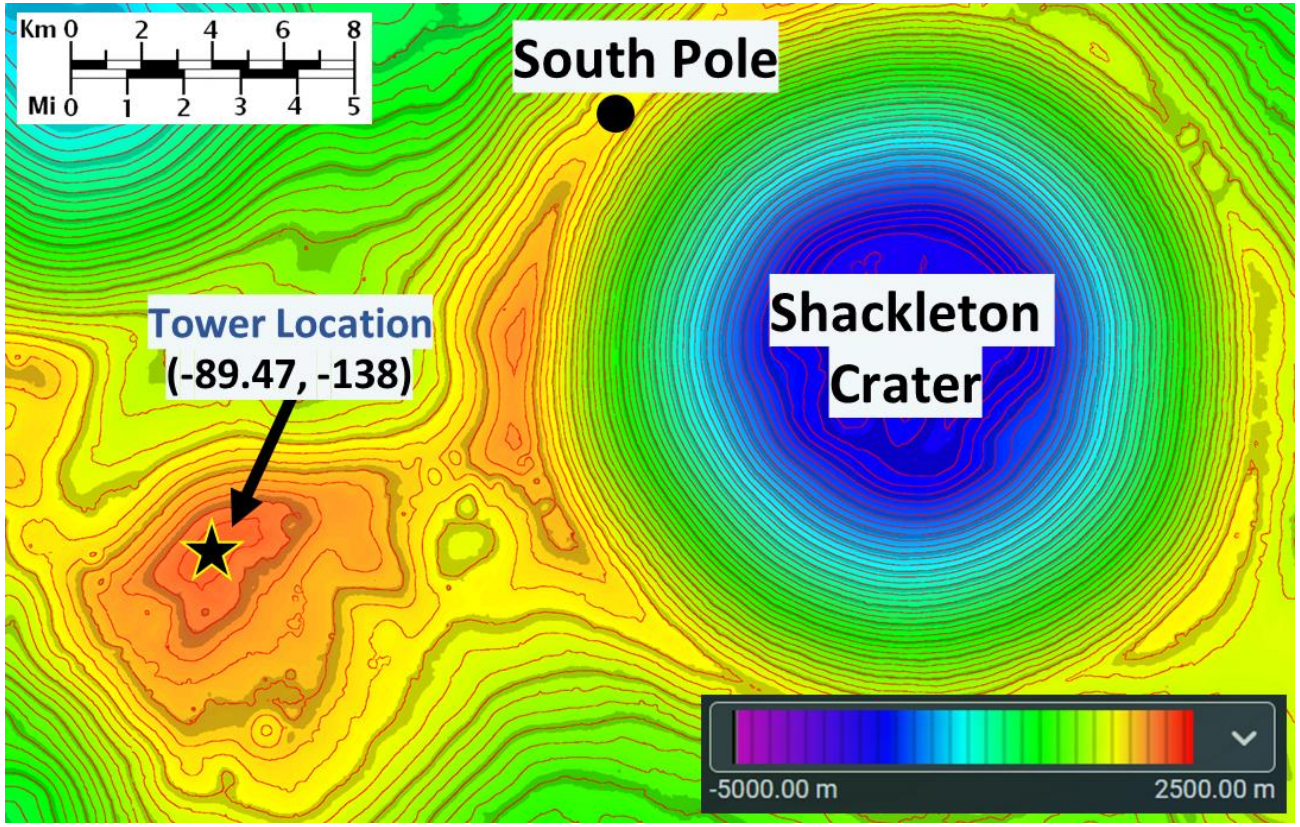

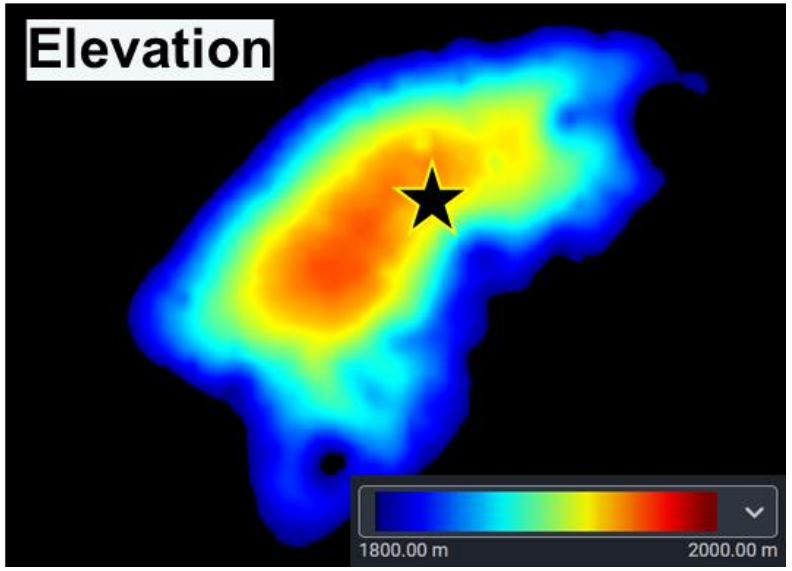

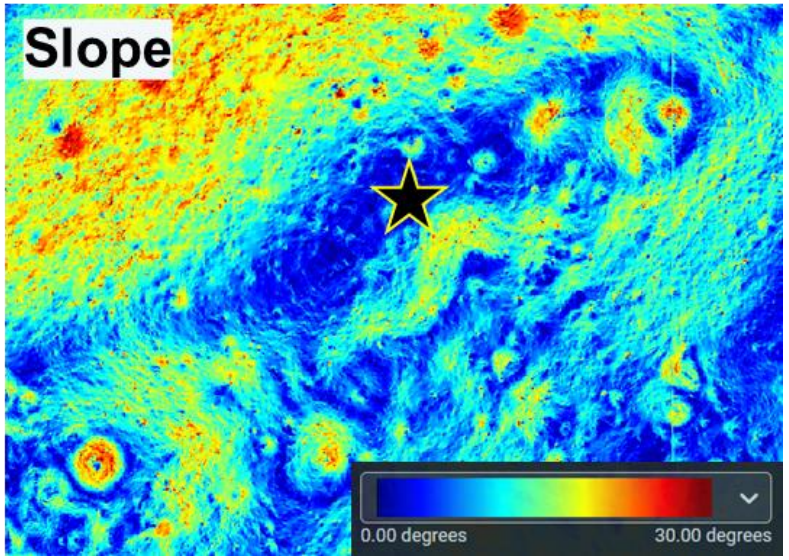

Note: Images from LRO QuickMap[8]

Lunar South Pole - Orbital

- Solar flux is primary heat load imparted on surface and tower
- Vector orbit and time varying solar flux from JPL Horizons[11]
- Solar vector stays relatively in-plane with horizon (long shadows)
- Solar diameter (subtended) angle included as constant 0.53º [4]
- Neglecting earthshine (0 to 0.15 W/m²) and eclipses (~hours)[4]
- Investigated date range: 6/1/2025 to 6/1/2026

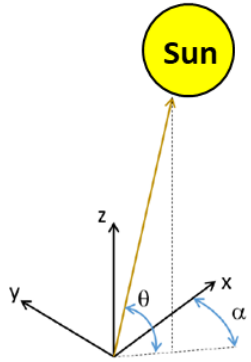

$$\theta = Elevation\ Angle$$

$$\alpha = Azimuth\ Angle$$

$$\vec{v} = (cos\theta_a cos\alpha)\hat{\imath} - (cos\theta_a sin\alpha)\hat{\jmath} + (sin\theta_a)\,\hat{k}$$

$$Planet\ Vector = (0,0,-1)$$

Vector Translation[4]

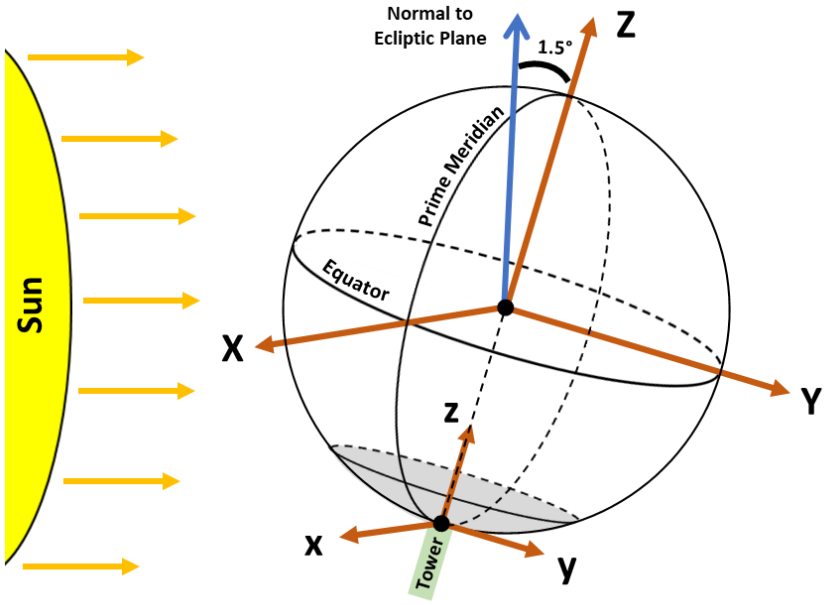

Lunar Geometry and Coordinate Axes

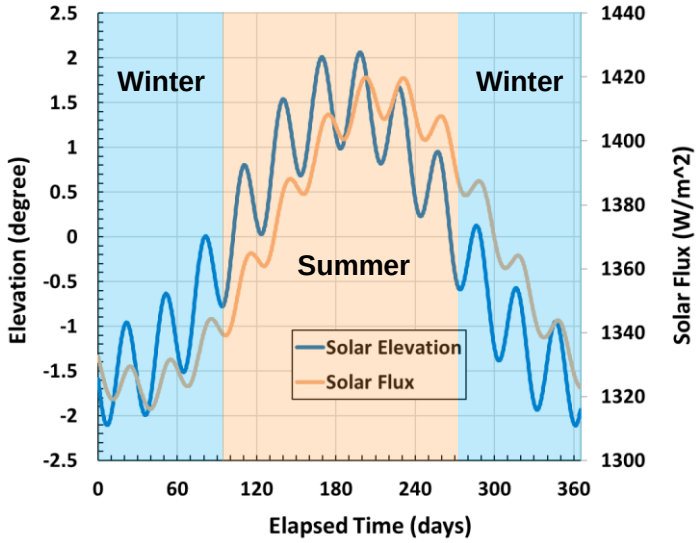

Solar Path and Flux

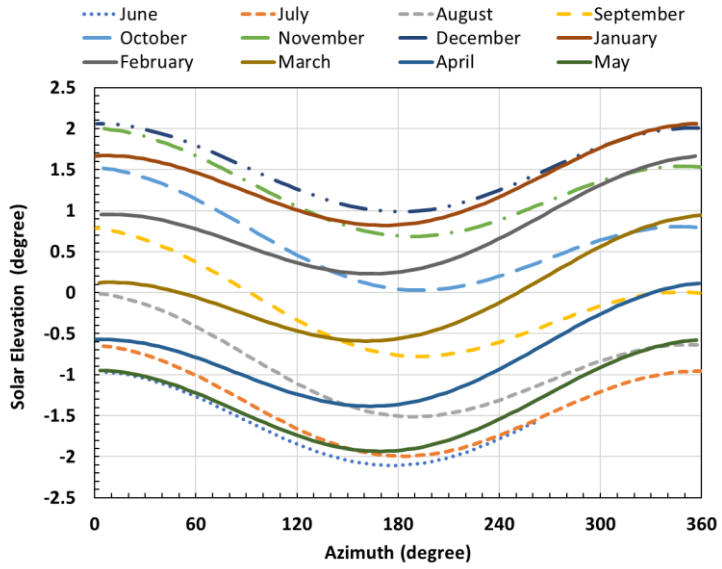

Solar Path by Month

Lunar South Pole - Surface

- Surface properties defined from DSNE and LTAG[3,4,12]
  - IR emissivity, solar absorptivity, albedo[3]
  - Depth dependent density[13,14]
  - Depth and temperature dependent thermal conductivity[13-15]
  - Temperature dependent specific heat[16]
- Not included in thermal model
  - Incident angle dependent optical properties[17,18]
  - Subsurface ground heat flow (~0.018 W/m²)[12]
  - Regolith dust migration onto tower

Surface Optical Properties:	
Property	**Value**
IR Emissivity, ε	0.965
Solar Absorptivity, α	0.840
Albedo	0.160

Surface Stacked Layer Properties				
Layer	**Thickness [m]**	**Density, [kg/m³]**	**Thermal Cond. [W/m/C]**	**Specific Heat [J/kg/C]**
1	0 to 0.02	1198	Temperature and Depth Dependent (see plot)	Temperature Dependent (see plot)
2	0.02 to 0.04	1348		
3	0.04 to 0.8	1506		
4	0.08 to 0.16	1673		
5	0.16 to 0.32	1774		
6	0.32 to 0.64	1798		
7	0.64 to 1	1800		
8	1 to 1.5	1800		

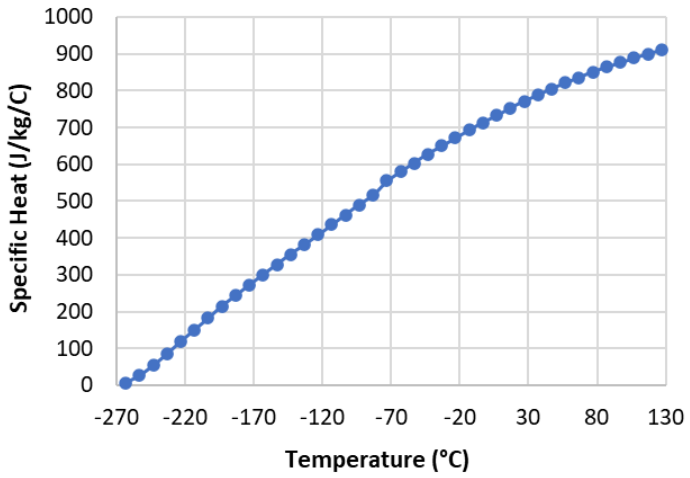

Specific Heat

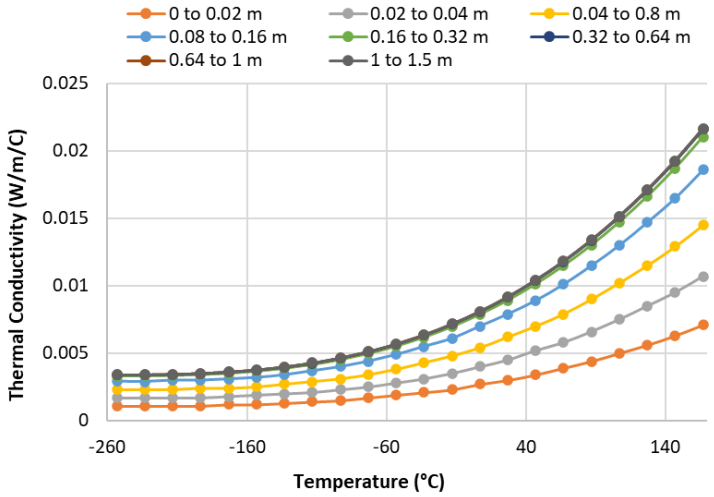

Thermal Conductivity

Flat Ground Plane Approximation

- Adequate for prediction of temperature and gradient extremes
- Flat plane doesn't accurately simulate temperature timeline
  - Incident solar illumination during winter months is obstructed
- Flat plane sized relative to:
  - Minimum solar elevation angle incident at top of tower
  - Lunar radius and average local terrain elevation
  - Lander (separation distance) and tower height

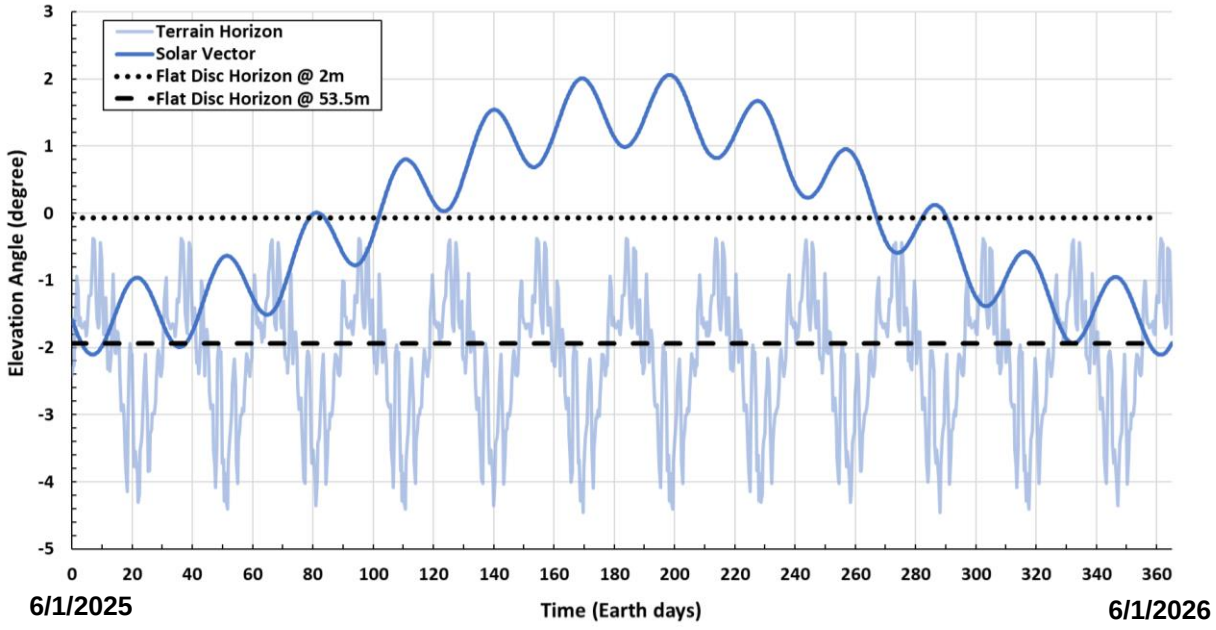

Flat Plane vs Terrain and Solar Path

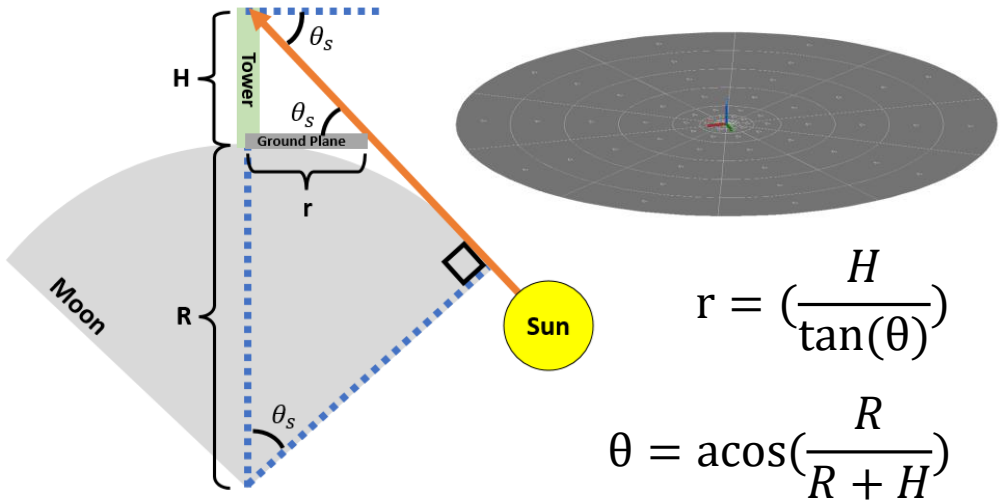

$$r = \left(\frac{H}{\tan(\theta)}\right)$$

$$\theta = \operatorname{acos}\left(\frac{R}{R+H}\right)$$

Parameter Title	Symbol	Unit	Value
Lunar Radius	R	Meter	1737000
Tower Height	H_1	Meter	51.5
Local Elevation	H_2	Meter	1937.83
Lander Height	H_3	Meter	2
Surrounding Terrain Height	H_T	Meter	1000
Minimum Solar Elevation Angle	θ_s	Degree	1.936
Surface Plane Radius	r	Meter	1583

Flat Ground Plane Sizing

Lunar Surface Mesh

- Temperature results greatly influenced by site specific local terrain effects
  - Incident solar flux is dominant heat source and dependent on terrain horizon
- LOLA Digital Elevation Model (DEM) simplified for Thermal Desktop
  - Method and tools derived from LTAG sources[4,19,20]
  - Input DEM is -85º to the south pole (40 m/pxl), includes surface curvature[21]
  - Mesh simplified relative to points along horizon occluding min solar elevation

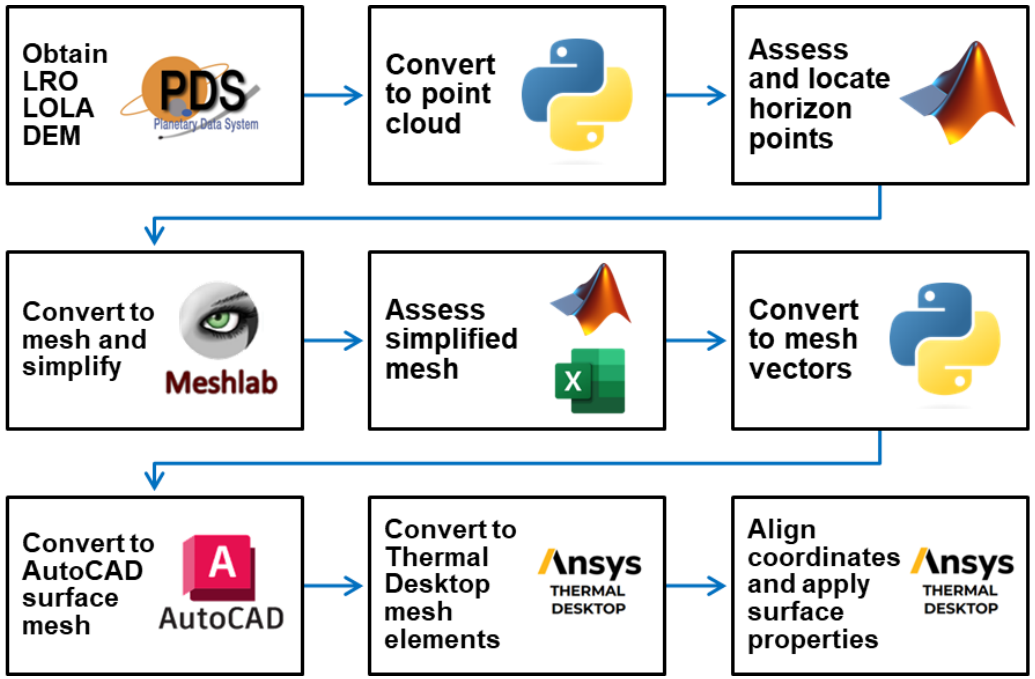

Lunar DEM Utilization Process[19,20]

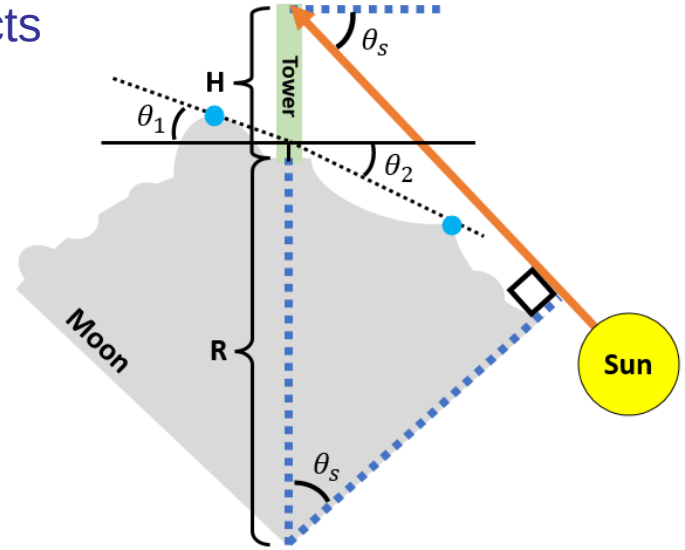

2D Lunar Terrain Diagram

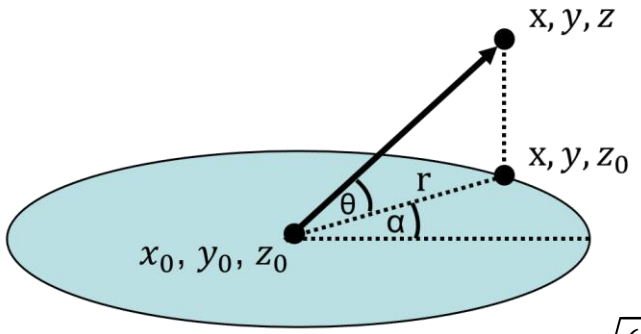

$$\alpha = tan^{-1}\left(\frac{y - y_0}{x - x_0}\right)$$

$$\theta = tan^{-1}\left(\frac{z - z_0}{r}\right)$$

$$r = \sqrt{(x - x_0)^2 + (y - y_0)^2}$$

Horizon Elevation Calculation

Lunar Surface Mesh

- Horizon elevation vs azimuth plot obtained via methods matching those found in literature[22-27]
  - Differences between horizon trends in plots below are due to inverse x-axis progression for azimuth and time
- LRO DEM converted to point cloud and analyzed in MATLAB
  - Calculates and plots horizon elevation across azimuth range in 1º increments from tower location
  - Sun position obtained from JPL Horizons over date range for specific tower location
  - Accounts for tower separation height from lunar surface (2 meters)

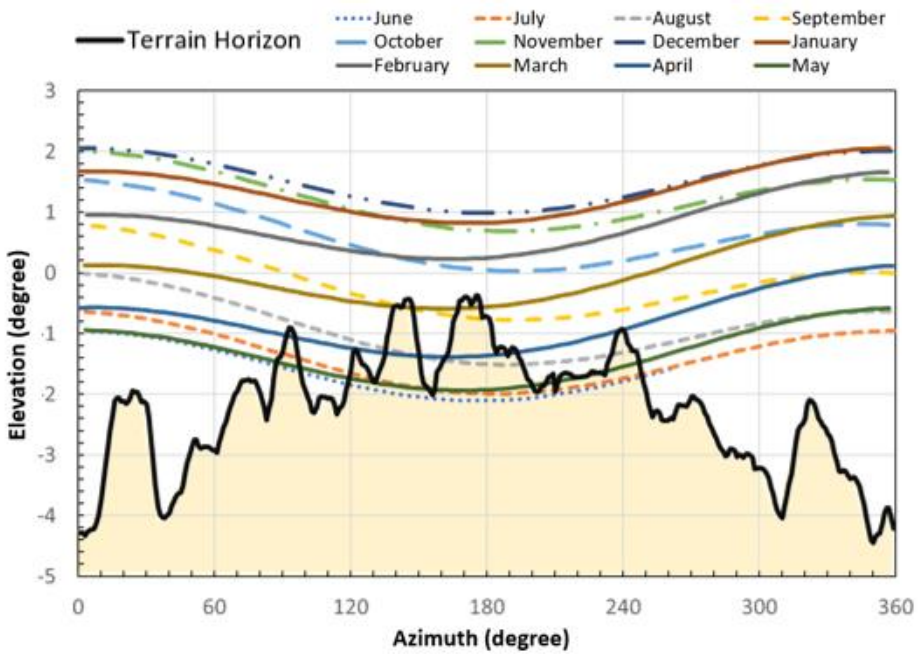

Calculated Horizon Plot (MATLAB)

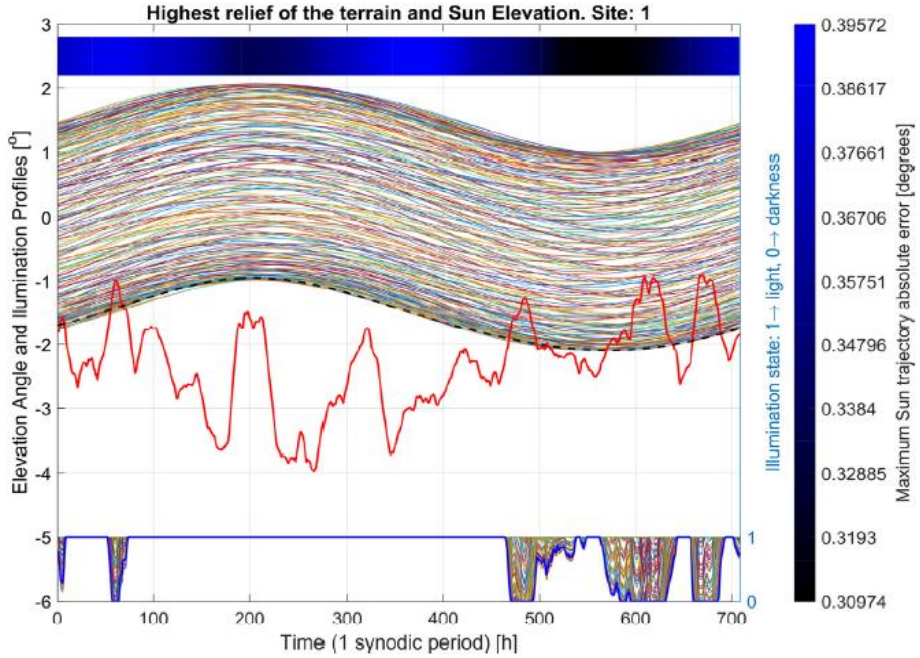

Literature Horizon Plot[27]

Lunar Surface Mesh

- Simplified mesh for Thermal Desktop
  - High mesh density at points along horizon intersecting minimum solar elevation angle path
  - Low mesh density at locations not intersecting solar path
  - 15% Root Mean Square Error (RMSE) at sunlit regions of interest for 15,000 node mesh surface

Title	Comment	RMSE Sunlight Points	RMSE All Points	Vertices Count
85°S DEM	40 m/pxl	Datum	Datum	57,000,000
P10	Unedited	10%	10%	1,290,000
P9	Unedited	18%	15%	320,000
P8	Unedited	25%	22%	79,000
P7	Unedited	34%	37%	20,000
15k	**Selected Regions**	**15%**	**35%**	**15,000**

LRO DEM[18] **Point Cloud**

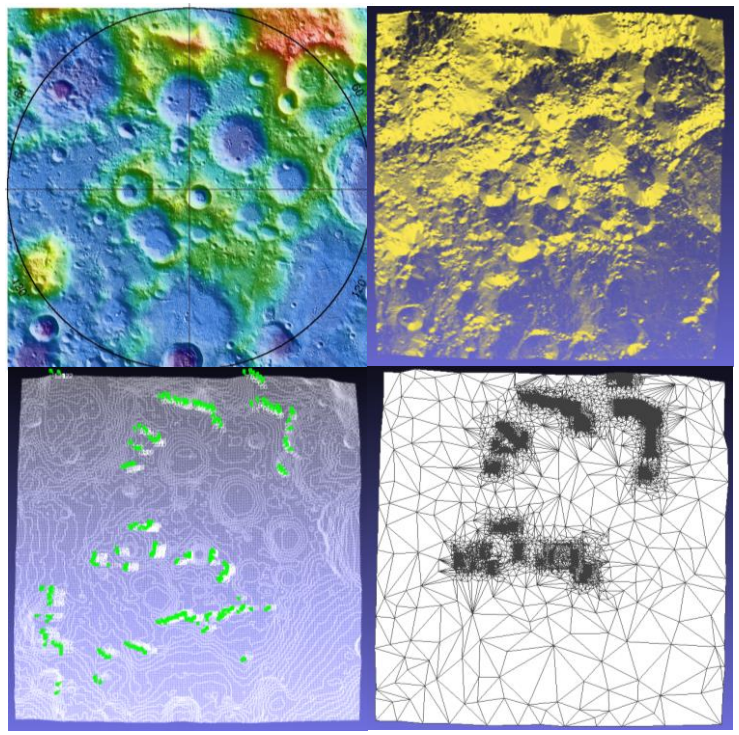

Fine Mesh **Reduced Mesh**

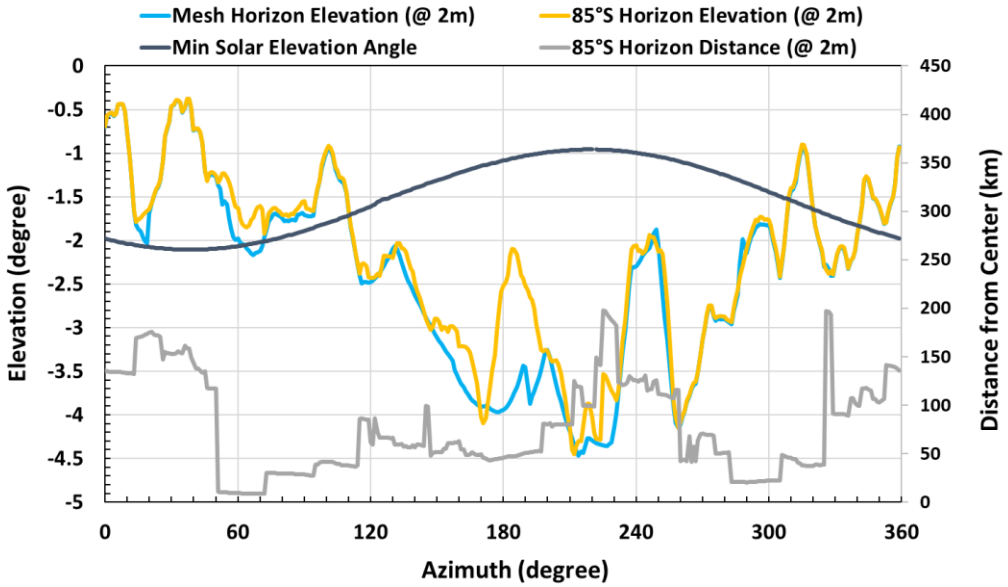

Horizon Elevation Plot

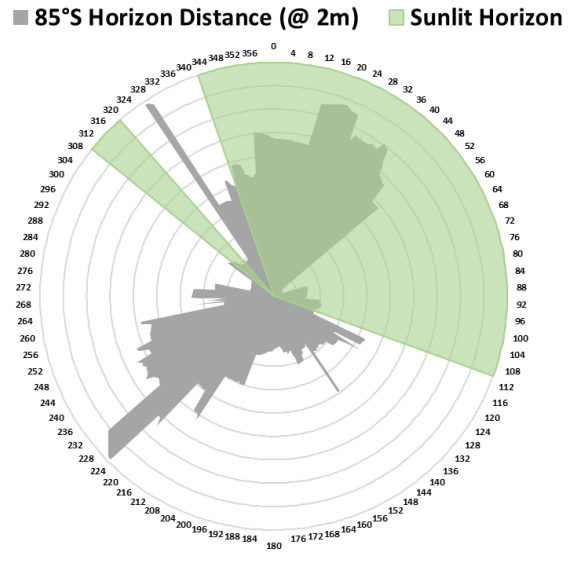

Horizon Radial Distance

Tower and Surface Simulation

- 40-to-200-day simulation shown with time steps of 30,000 seconds
  - 3.5 Earth days per second of video, ○ = tower location

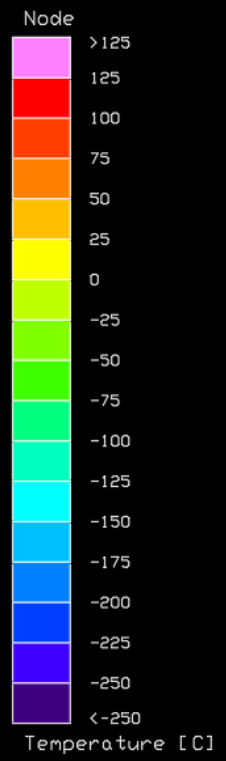

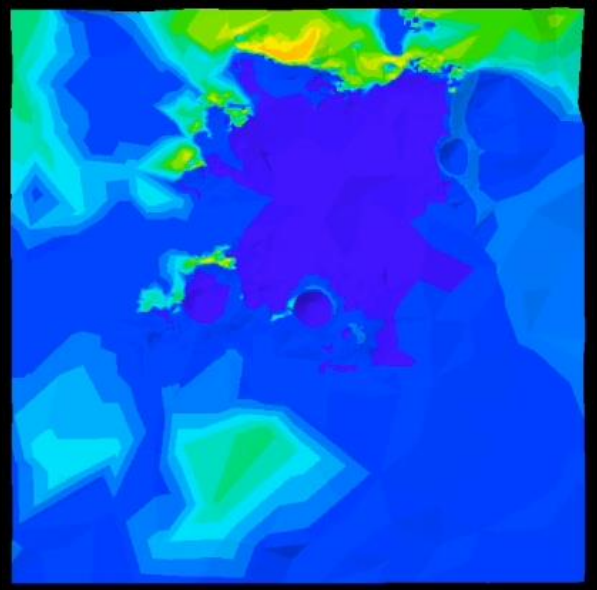

-85º from South Pole

Shackleton Connecting Ridge

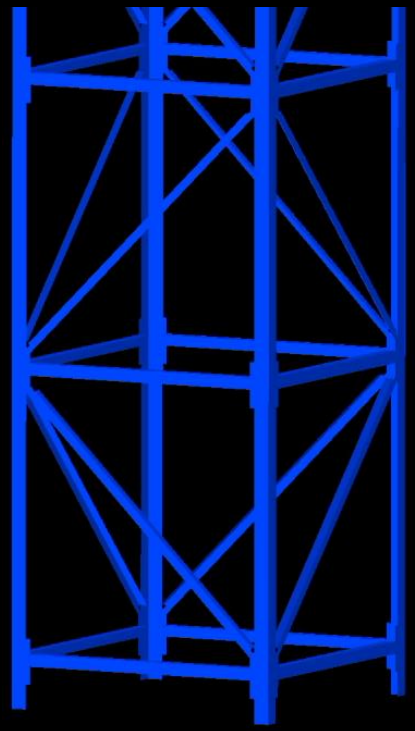

Tower Base

Tower Base

Tower Top

Terrain vs Solar Path

- Thermal Desktop produced temperature trend matches terrain horizon vs solar illumination
  - Results verified via inspection with LRO QuickMap Viewer[8]
  - Thermal model mesh and LRO DEM horizons shown for comparison

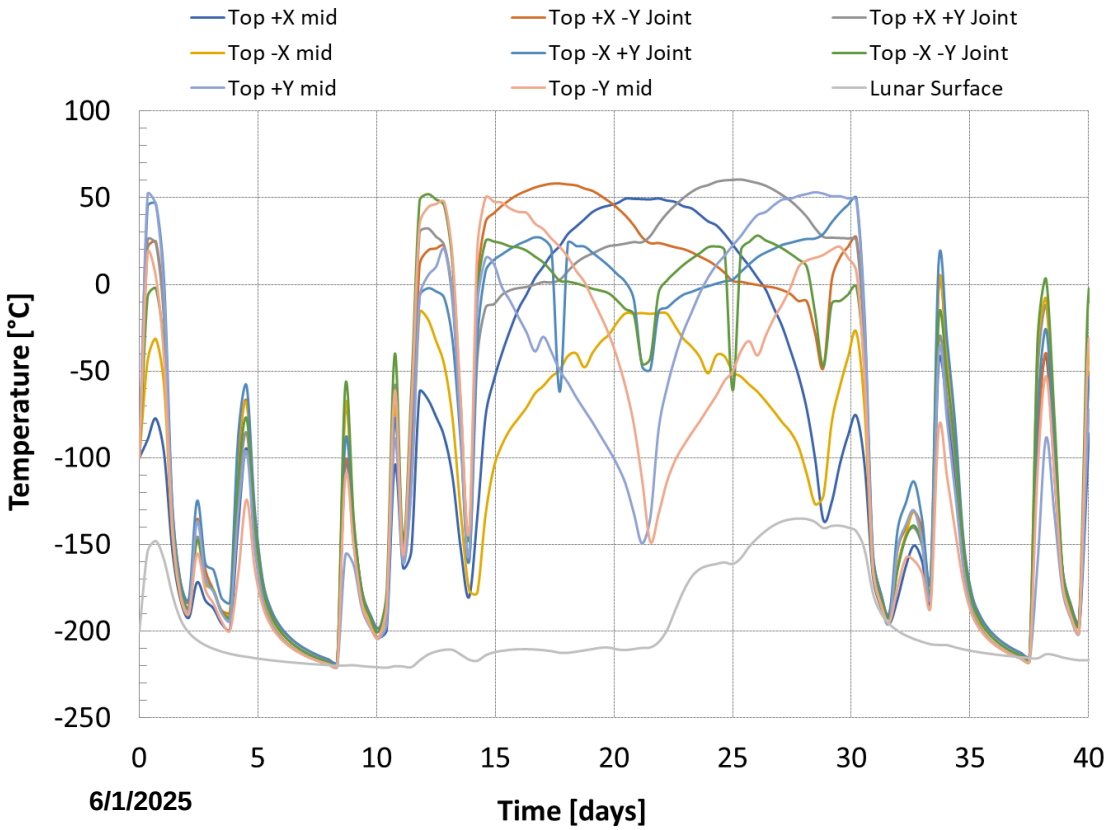

Top of Tower Temperature

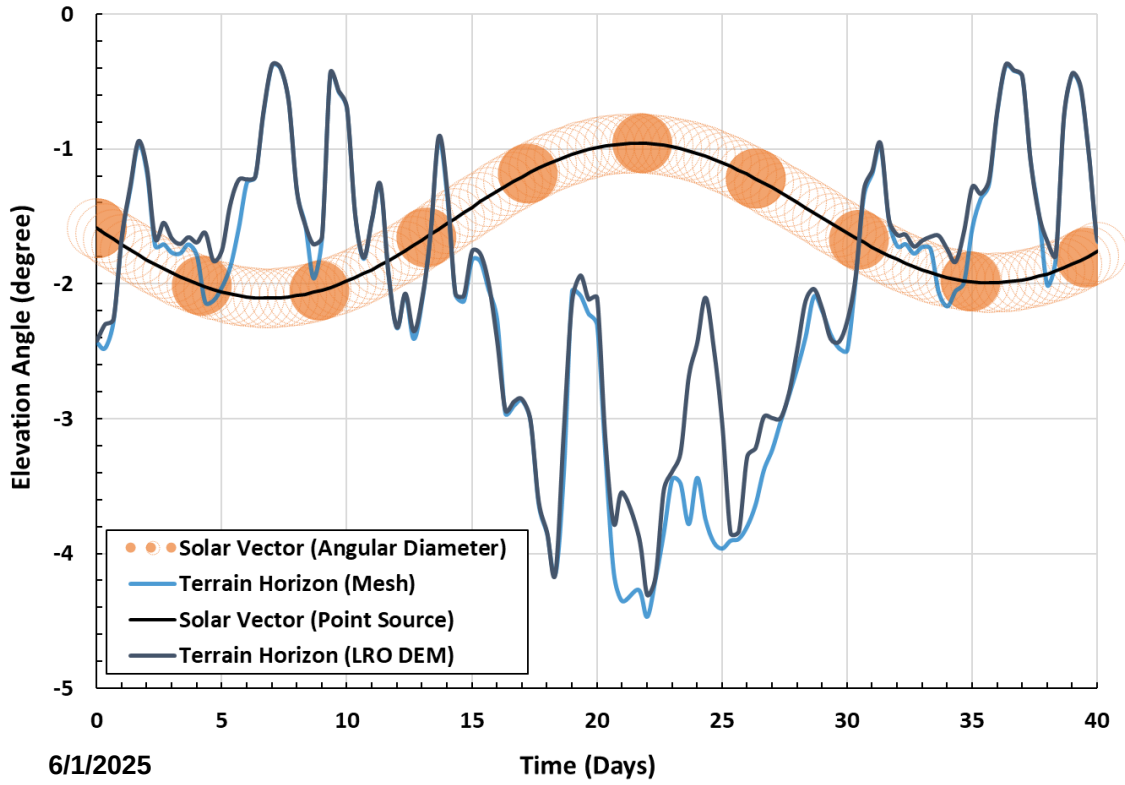

Terrain Horizon and Solar Path

Tower Temperature Results

- Temperature values do not include design or test margin
- **Min Temperature:** -228ºC at diagonal member midsection
- **Max Temperature:** 75ºC at joint diagonal tab
  - Well below material glass transition temperature of 140ºC [9]
- Significant gradients across tower height and cross section
  - Large fluctuations and gradients caused by cross member shadowing

Gradient Temp. [Δ°C]	From Location [x, y, z]	To Location [x, y, z]
269	(+x, 0, 0)	(+x, 0, 51m)
257	(-x, 0, 0)	(-x, 0, 51m)
132	(+x, +y, 27m)	(-x, -y, 27m)

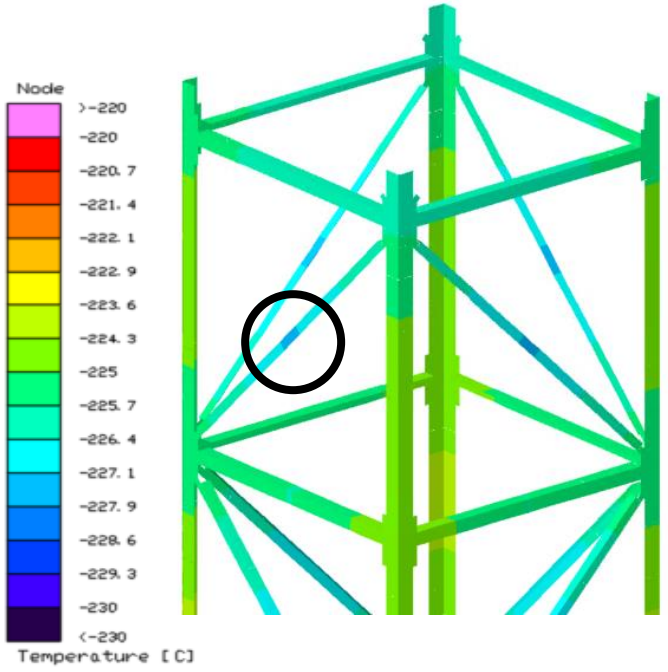

Minimum Temperature

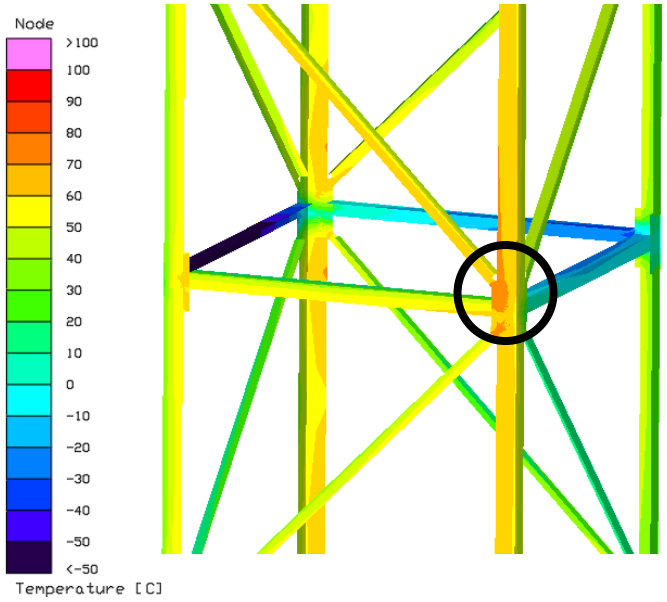

Maximum Temperature

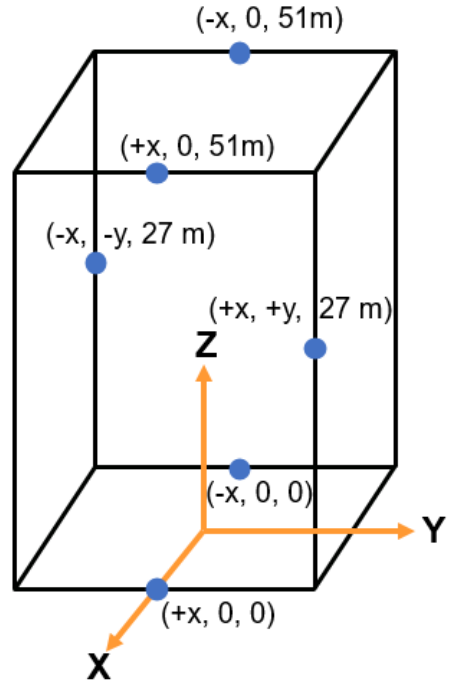

Maximum Gradients

Tower Temperature Measures

- Temperatures trends recorded at each joint and horizontal element midsection for (1) base, (2) middle, and (3) top of tower
  - Eight measurement points at each height
- Additional measures placed on top and bottom joints of base RUC to capture trends at possible weld locations

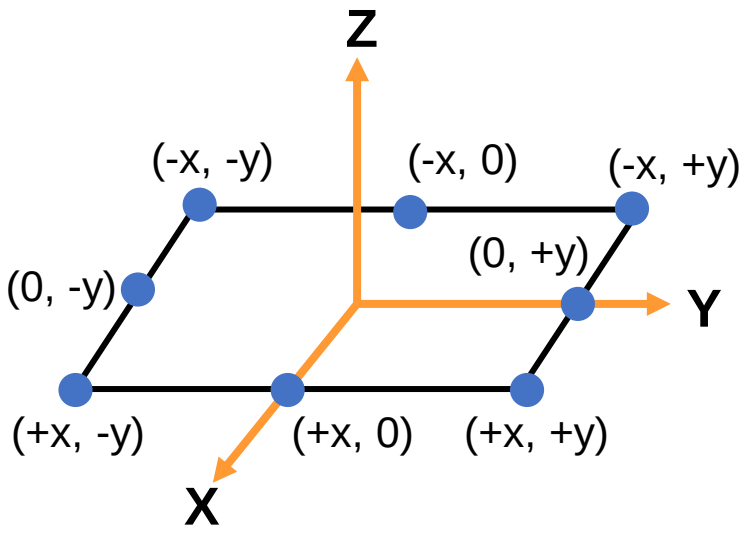

● = Measurement Point

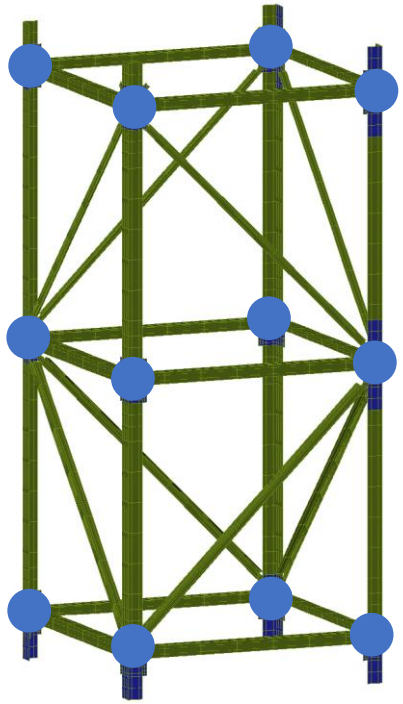

Base RUC Joint Measures

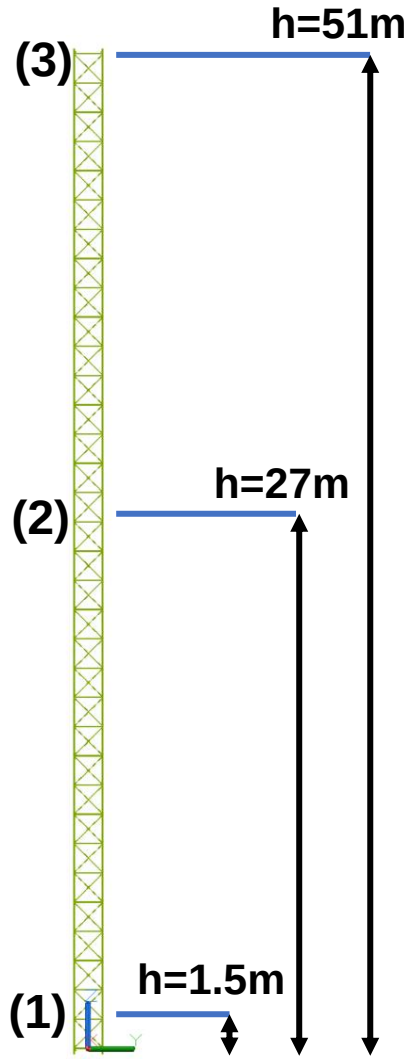

Tower Gradient Results: 0 to 365 days

- Horizontal gradients vary cyclically and are more severe during summer seasons
  - Caused by cross member shadowing, fluctuates radially as sun moves across horizon
- Vertical gradients are severe during winter and minimal in summer
  - Partial tower illumination (top of tower illuminated while base in shadow)

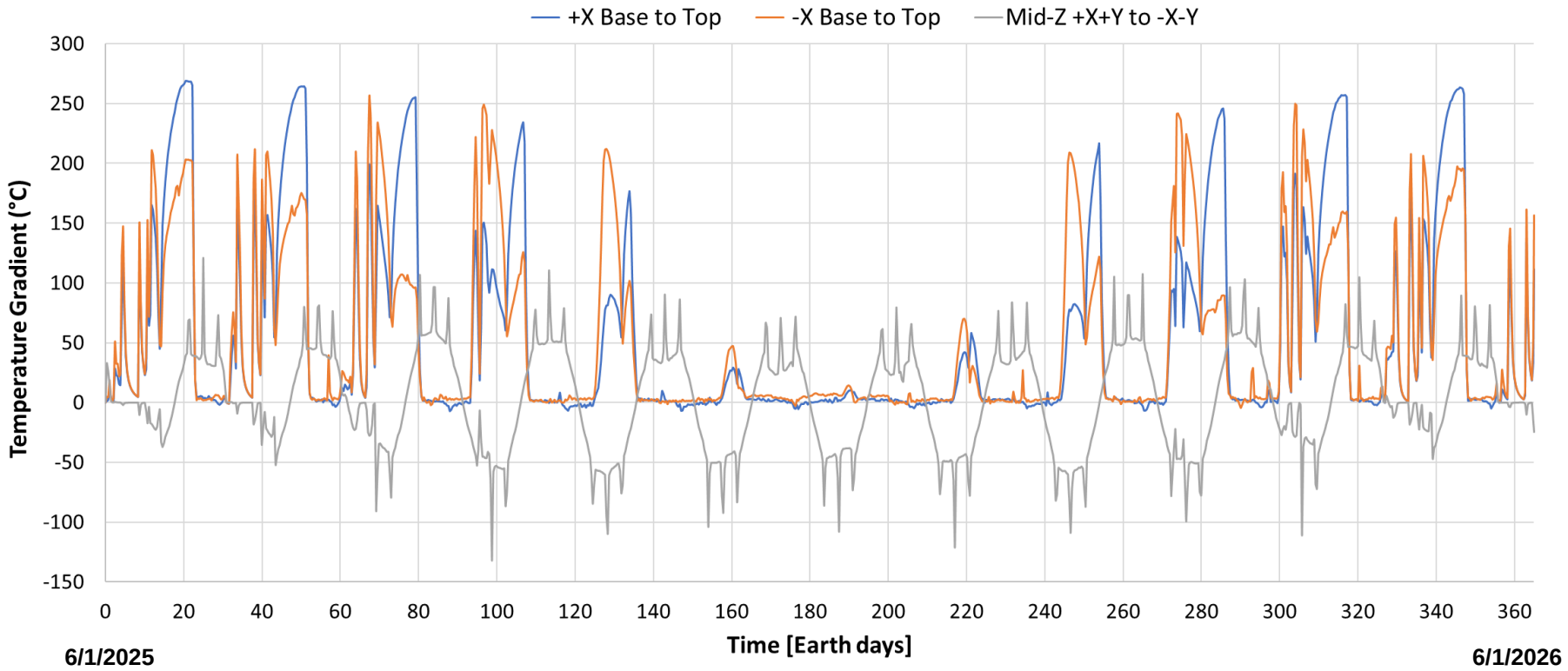

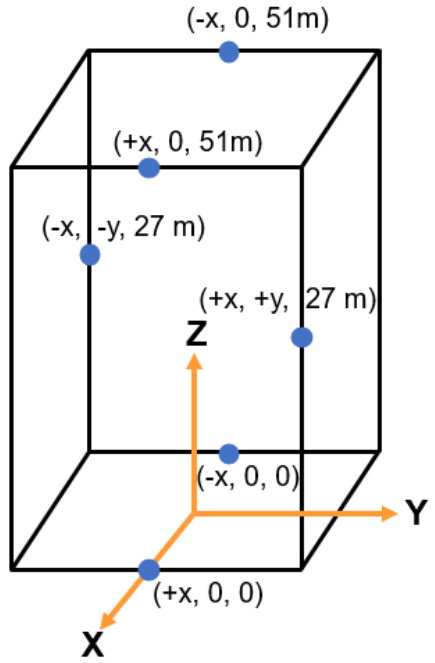

Tower Top Results: 0 to 365 days

- Near continuous solar illumination at top of tower (~85% of year)
  - Temperature variations caused mostly by cross-member shadowing (low solar elevation angle)
  - Maximum 4 days of total solar occlusion by terrain during winter season

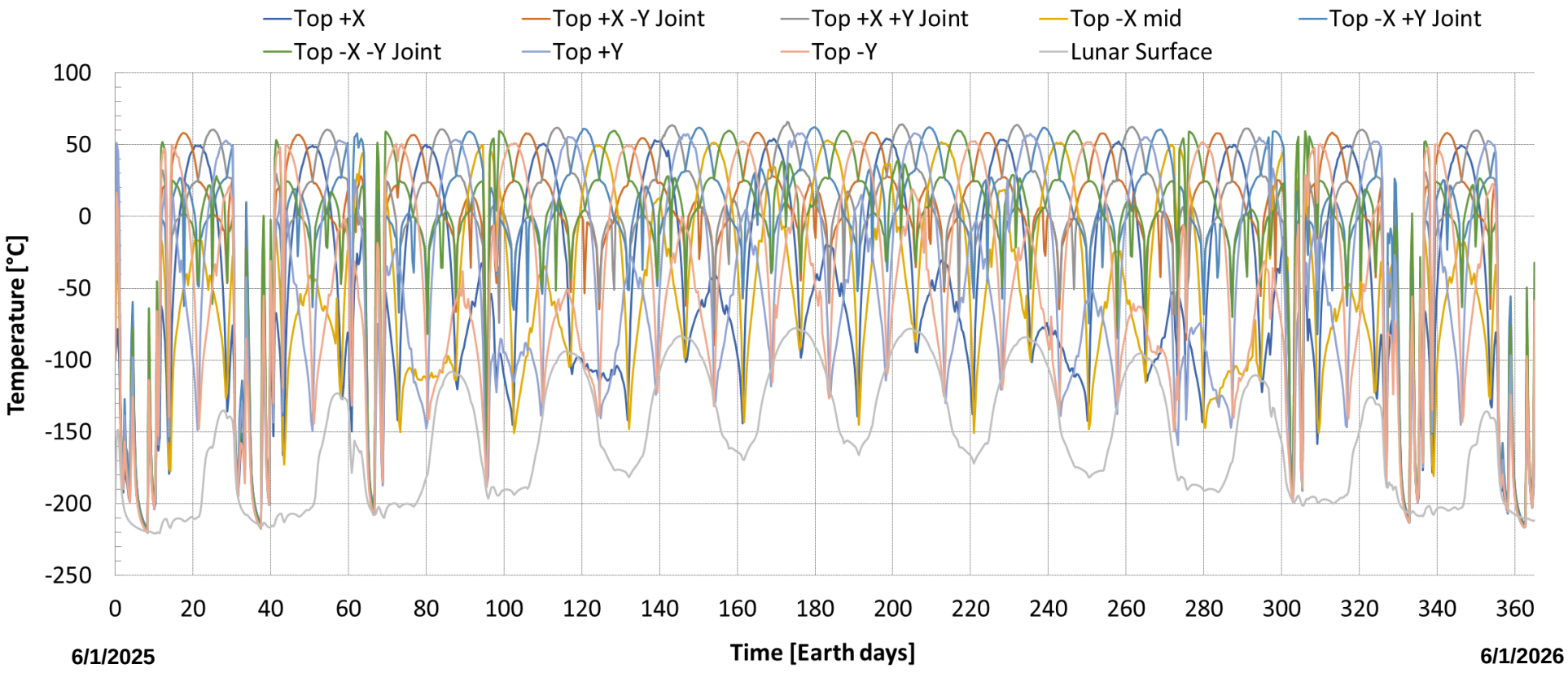

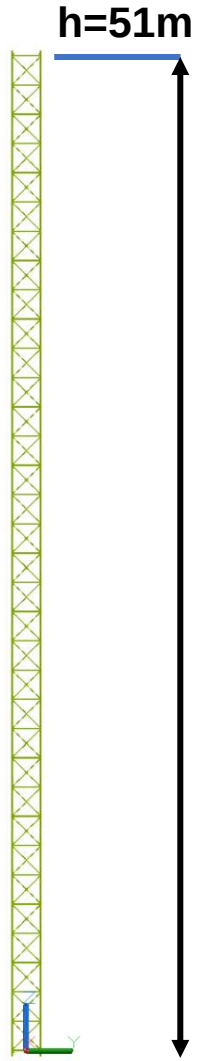

Tower Base Results: 0 to 365 days

- Partial solar illumination at base of tower (~50% of year)
  - Frequent drops to cryogenic temperatures caused by local ridge terrain occluding solar path
  - Tower base drops below lunar surface temperature in absence of solar illumination
  - Maximum total solar occlusion by terrain of 20 days during winter season

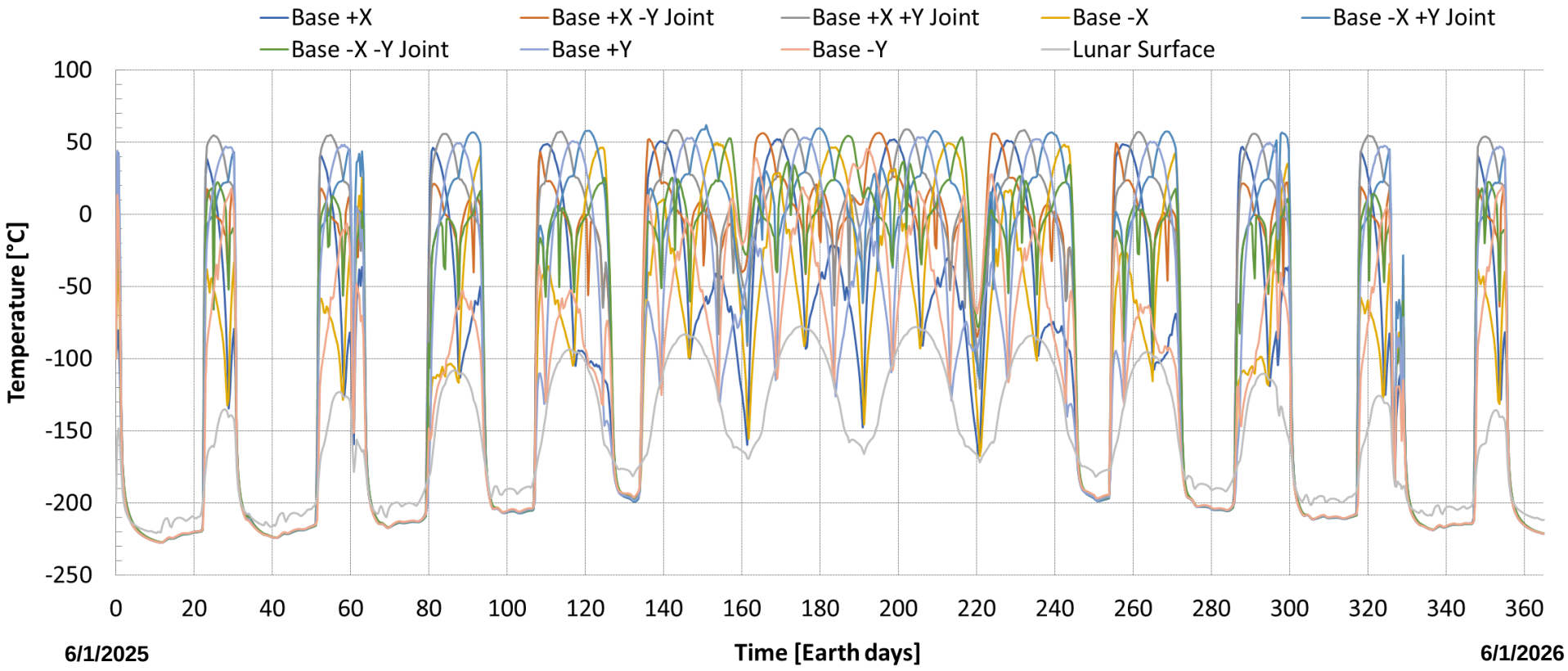

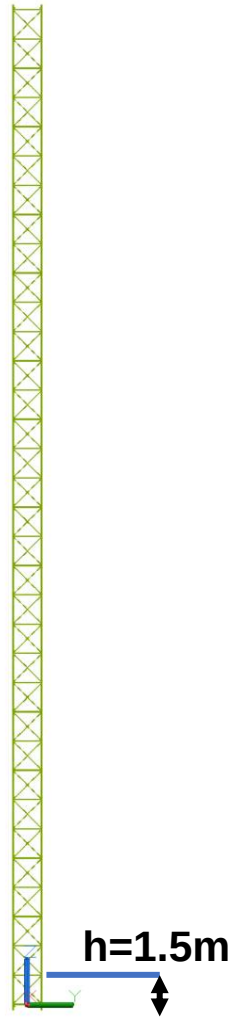

Bottom RUC Joint Results: 0 to 365 days

- Joints of bottom RUC where weld operations are likely to occur
  - Cross member shadowing impacts joint temperature less than horizontal members
  - Frequent drops to cryogenic temperatures caused by local ridge terrain occluding solar path
  - Minimum acceptable joint weld temperature impacts operations

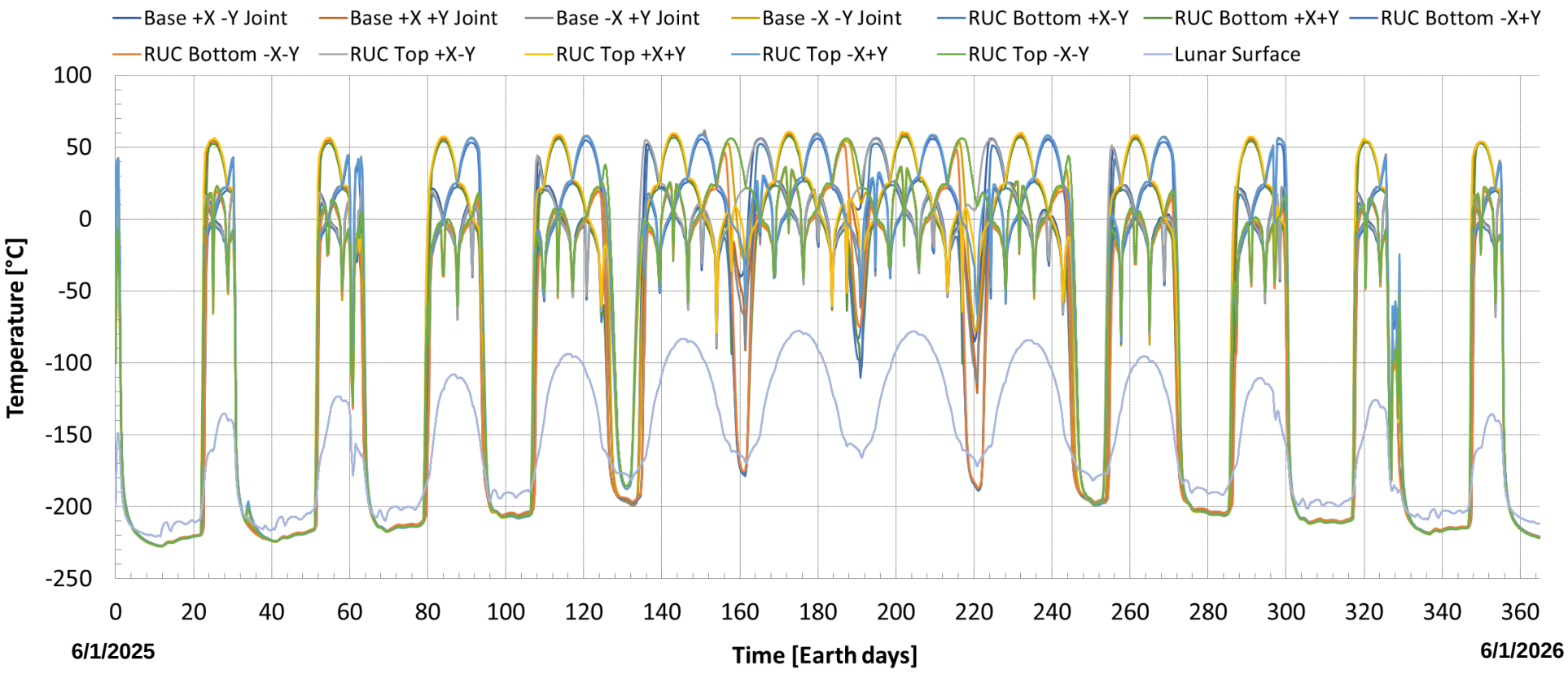

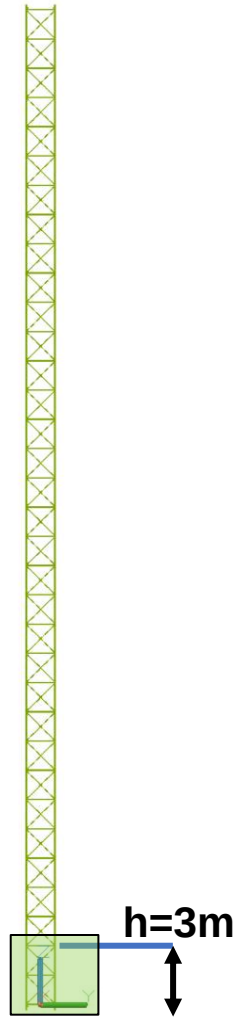

Joint Weldability Operations Study

- Varied minimum joint temperature as a design variable to predict duration for weld operations
  - Minimum acceptable weld temperature is currently unknown for selected process and material
  - Data represents periods where all joints of bottom RUC are above a specified temperature
  - Diminishing returns when minimum joint temperature values are colder than -70ºC

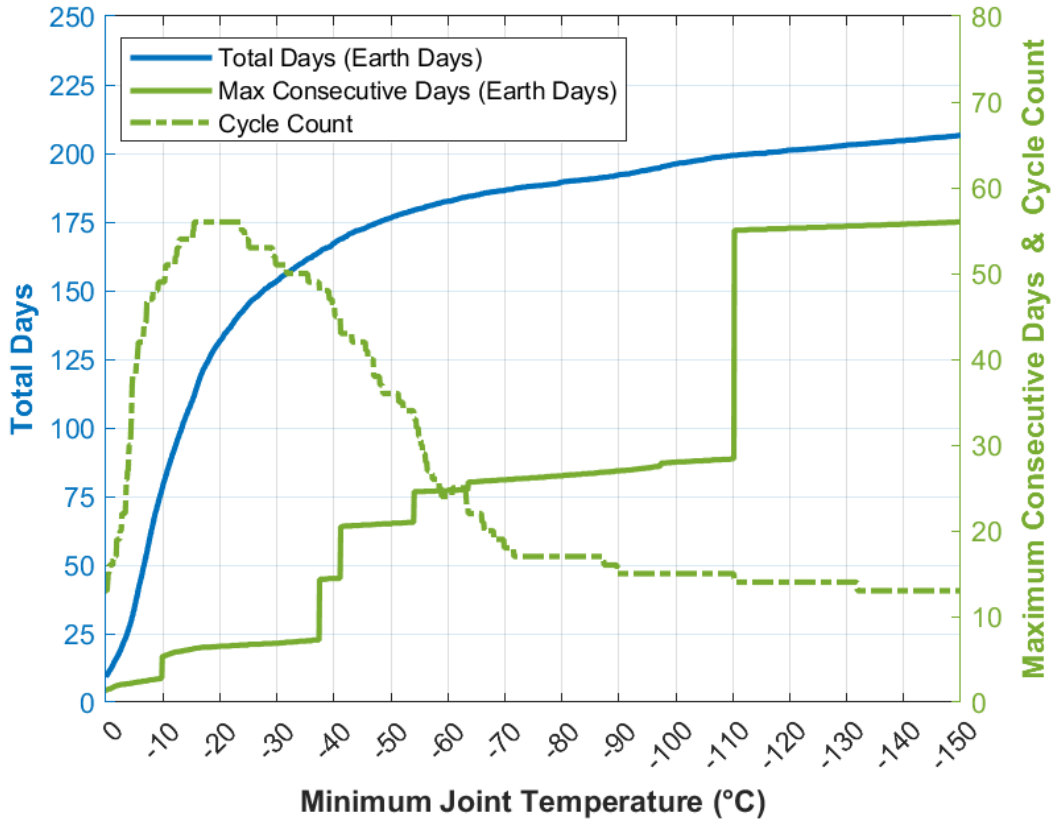

Operational Variables vs Joint Temperature

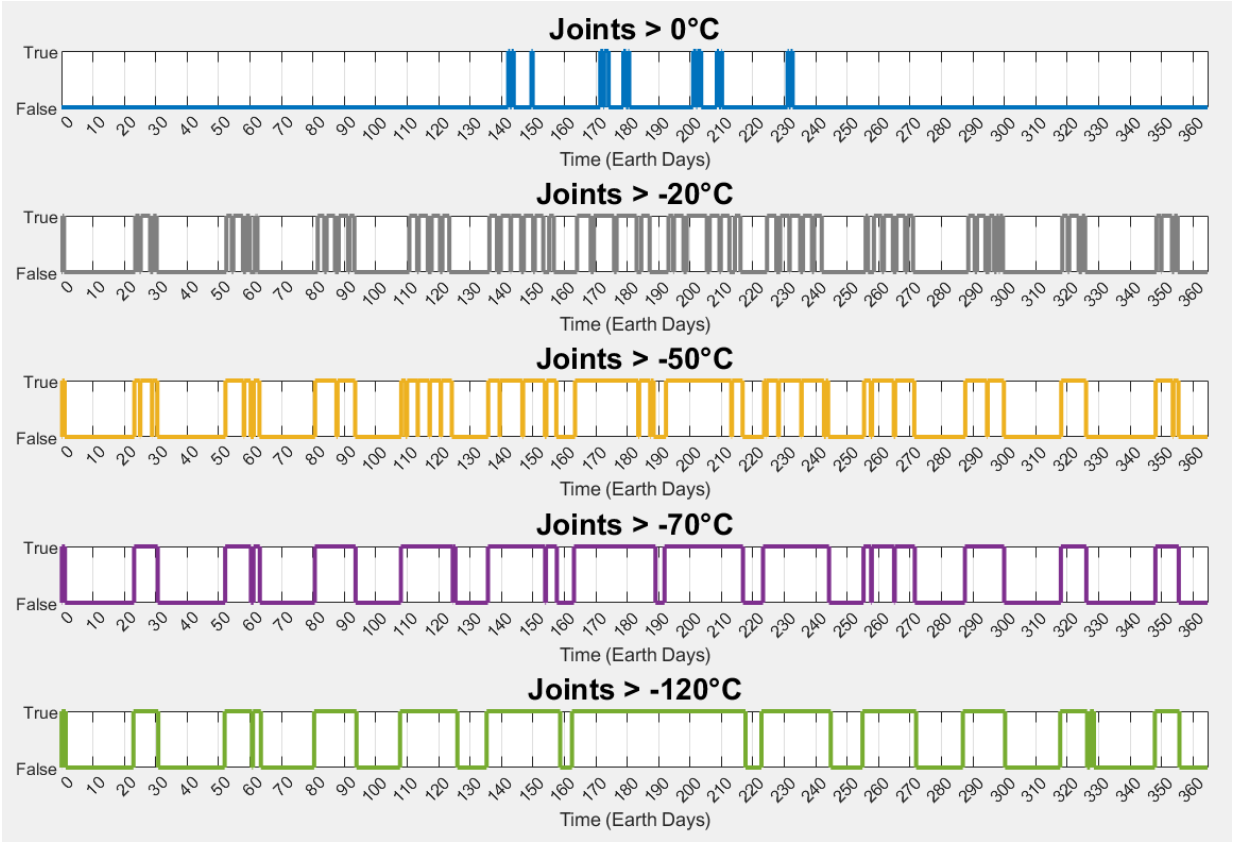

Joint Cycles vs Time (Earth days per year)

Thermal-Structural Deformation

- Timestep with large temperature gradients across loaded joints at tower base
  - Temperature values from thermal model mapped to structural finite element mesh with -180ºC initial temperature
  - Excluding residual/thermal stresses at welded interface and payload mass at top of tower
- Coefficient of Thermal Expansion (CTE)
  - Averaged (constant slope of strain vs temperature) CTE data from TDEA TC1225/T700 test report
- Maximum thermal displacement is small (0.76 cm)
  - High stresses observed at welded interfaces, especially at joints near lunar surface.
  - All welds show margin, but horizontal weld most susceptible due to mismatches in composite layups

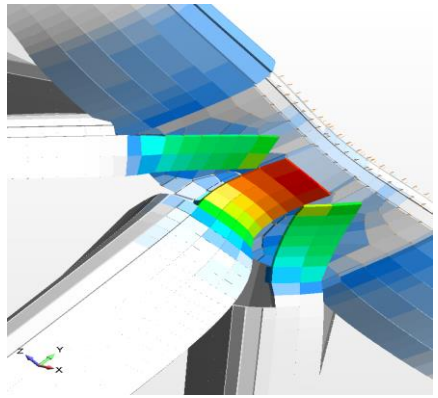

Joint Thermal Deformation

Structural portion of analysis performed by Babak Farrokh (GSFC-5420)

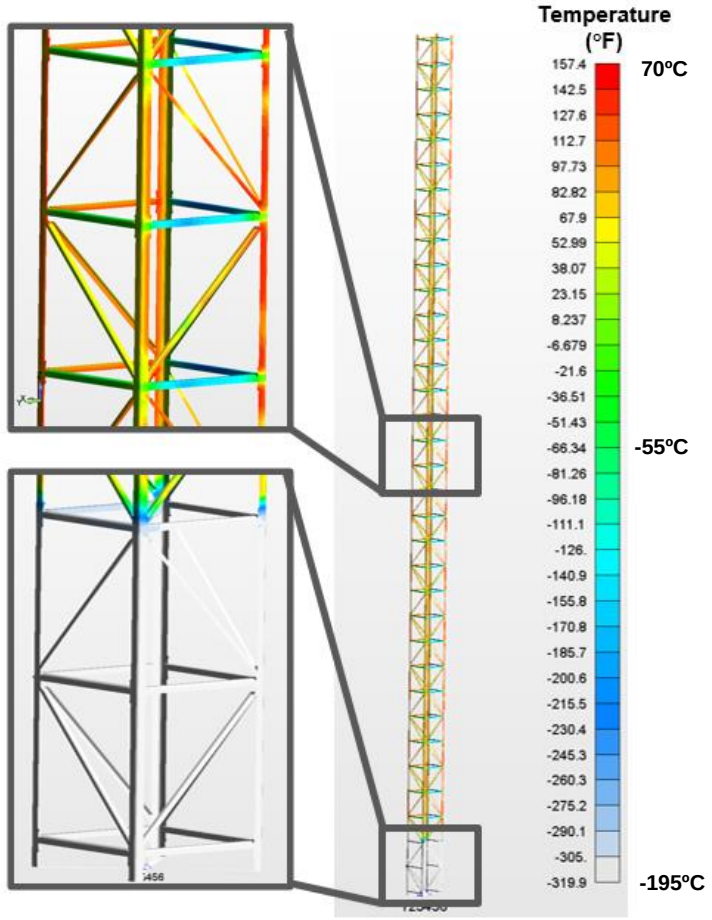

Selected Timestep

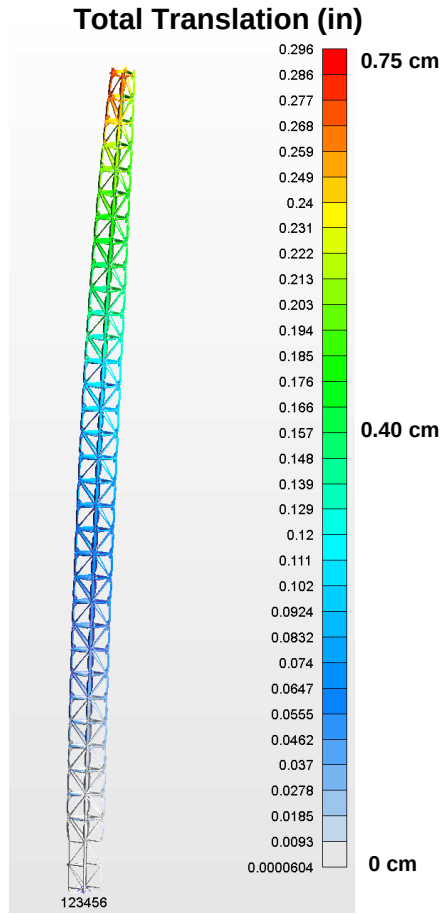

Global Tower Deformation

Property Sensitivity - Solar Diameter Angle

- Inclusion of solar diameter (subtended) angle affects thermal timeline results
  - Impacts results of winter months where partial solar occultation occurs frequently due to horizon interactions
  - Average tower temperature increases by 3ºC over 1 year

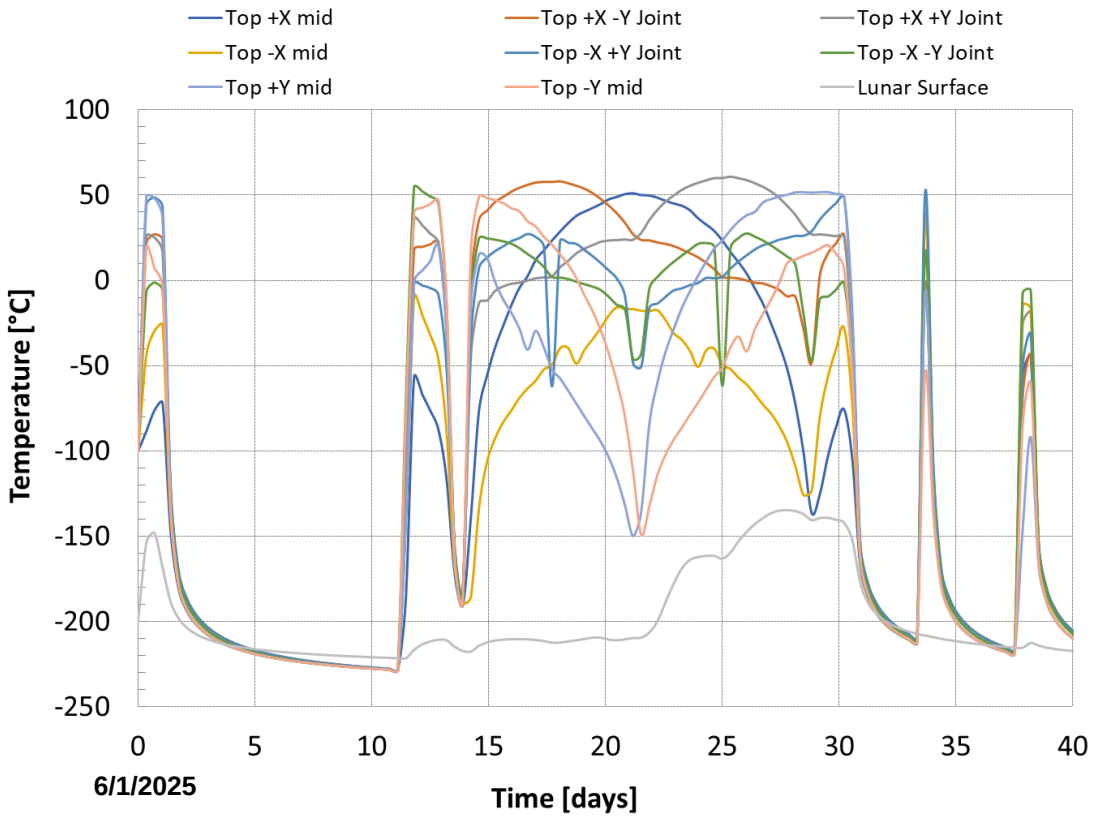

Top of Tower (Subtended Angle *Excluded*)

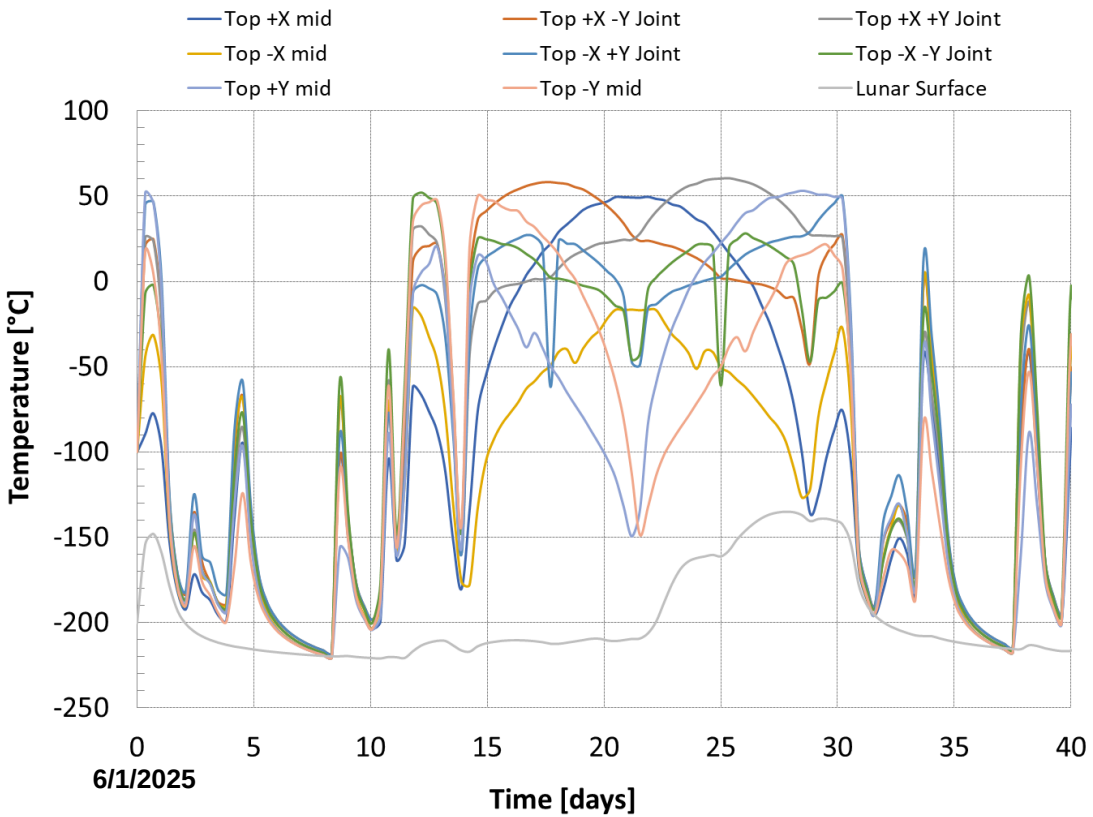

Top of Tower (Subtended Angle *Included*)

Property Sensitivity - Surface Temperature

- Seasonal average surface temperature plots derived from LRO data do not match predictions at specific location (-89.46752º, -138.012788º)[6]
  - Temperature values averaged from satellite measurements between 2009 and 2015[7]
  - Spatial data resolution is 240 m/pxl and temperature value error is ±5ºC [28]
- LRO seasonal average surface temperature trends are not sufficient to be used as boundary node assumption for this analysis
  - LRO trend does not represent the precise location coordinates due to low spatial resolution
  - LRO trend underpredicts and overpredicts hot and cold respectively due to averaging

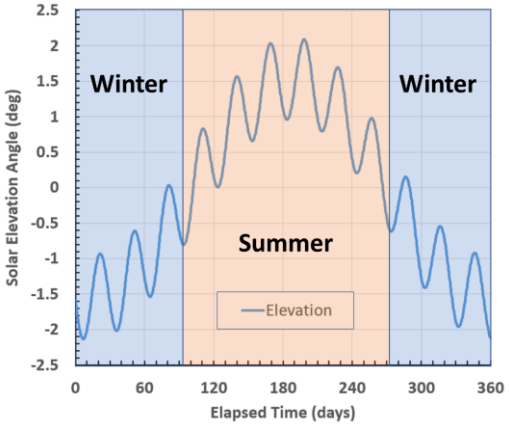

Lunar Seasons at Location

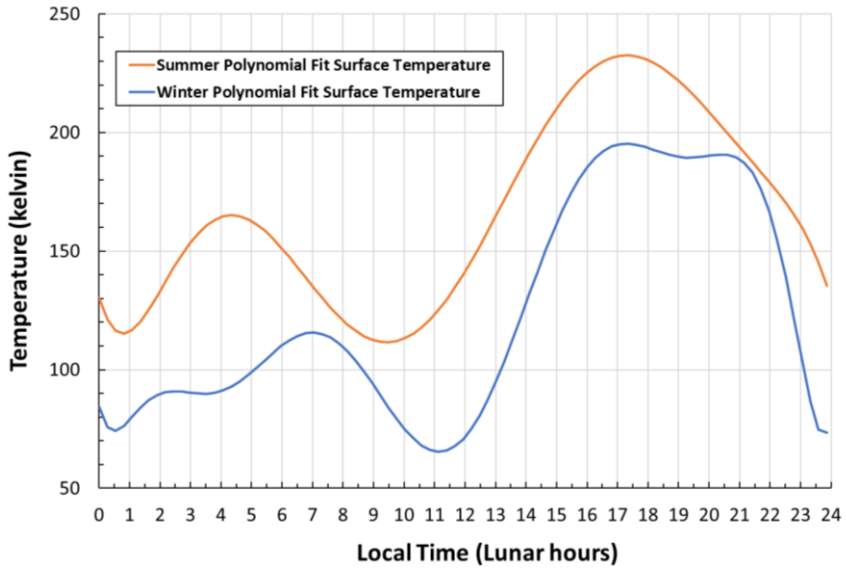

Seasonal Average Surface Temperature[6]

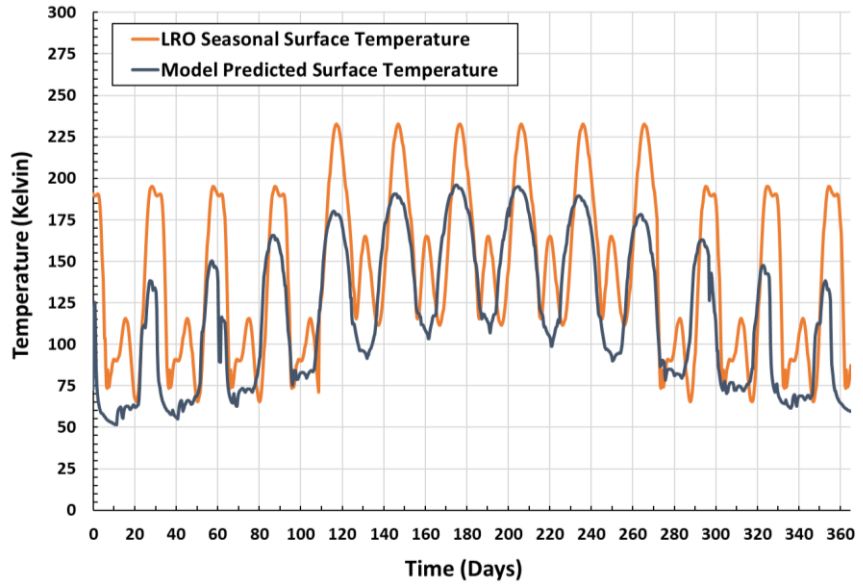

Surface Temperature - LRO vs Model

Property Sensitivity – Location and Surface Temperature

- Tower Location and terrain dependent surface temperatures
  - Solar illumination and surface temperature are extremely location sensitive. Precise coordinates necessary as latitude changes of .001 can alter location by ~100m
- Spatially sampled thermal model predicted surface temperature values
  - Temperature trends diverge outward from origin
    - Temperature trends along ridge (North and South) match closely
    - Trends differ Eastward and Westward due to terrain slope and elevation changes
  - Eastward maximum temperature occurs earlier in lunar day

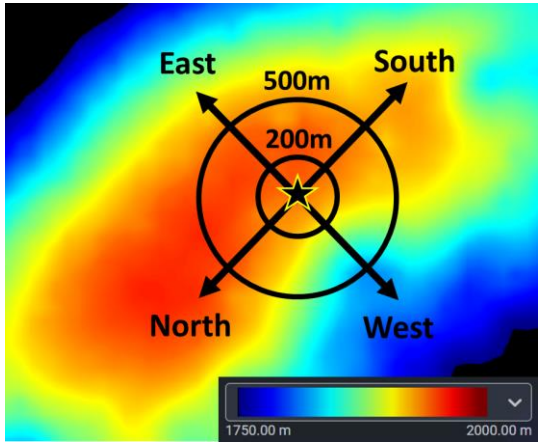

Site Elevation Map*

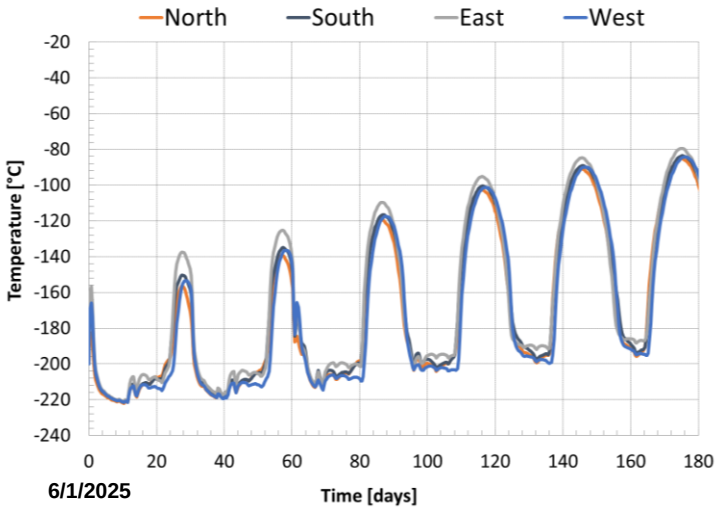

25m Directional Temperature

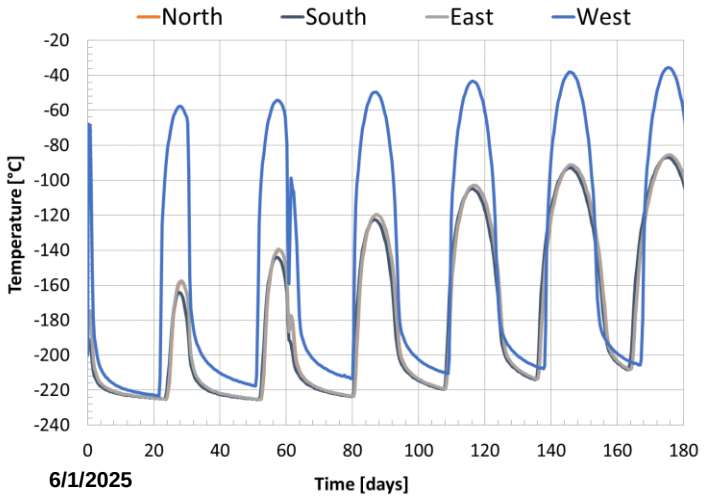

200m Directional Temperature

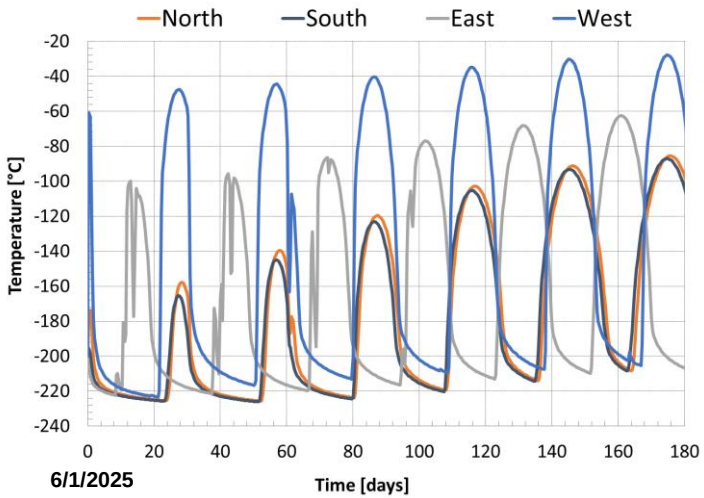

500m Directional Temperature

***Note:** Image from LRO QuickMap[8]

Property Sensitivity - Surface Temperature

- Gomez et al obtained 97.5% correlation between model predicted temperature and LRO data using the following properties[20]:
  - Solar absorptivity = Feng 2019 (incident angle dependent)[17]
  - Depth and thermal conductivity = Hayne 2017[14]
  - Specific heat = Woods-Robinson 2019[15]
- This analysis used the following properties:
  - Solar absorptivity = DSNE[3]
  - Depth and thermal conductivity = Hayne 2017[14]
  - Specific heat = Woods-Robinson 2019[15]
- DSNE optical properties predict higher surface temperature
  - Surface temperature differences between using DSNE and Feng 2019 optical properties negligibly affect tower temperatures

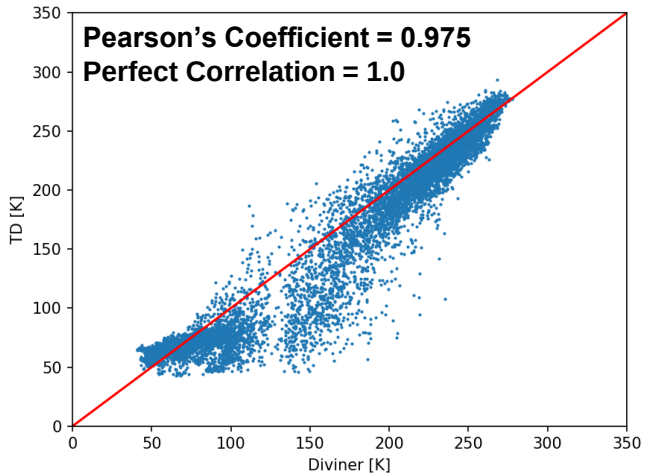

Scatter Density Plot[20,29]

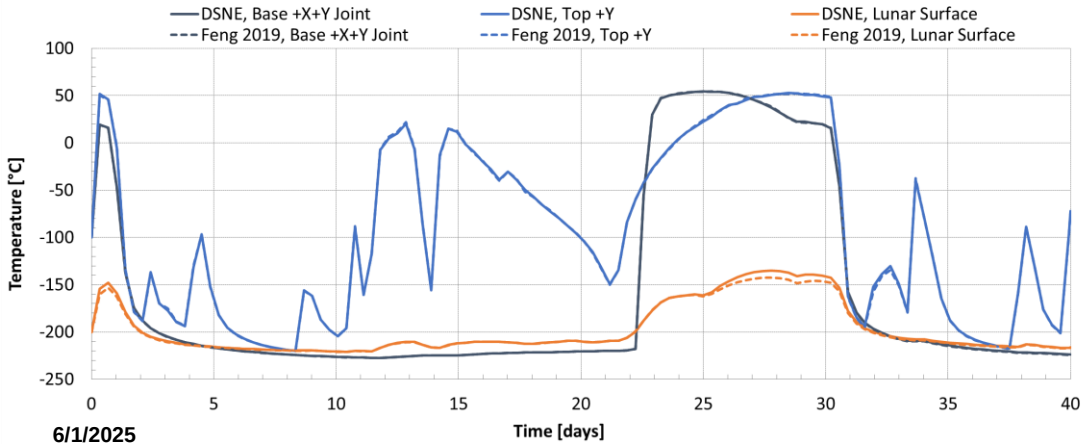

Tower Temperature, DSNE vs Feng 2019

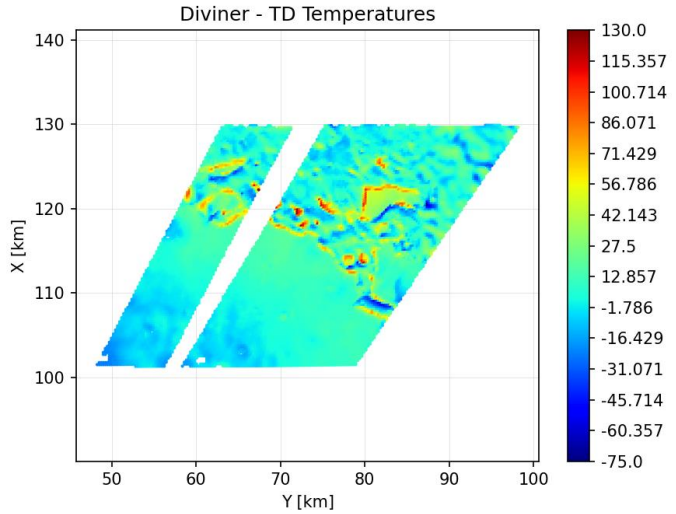

LRO vs Model Prediction[20]

Property Sensitivity – Tower Material

- Tower conductivity
  - Composite thermal conductivity significantly affects hot temperature results if changed by a factor of ≥2
    - Multiplying values by factors of 0.1x and 10x impact maximum temperature by +20ºC and -15ºC respectively
- Tower specific heat
  - Composite specific heat affects results transition to cold and associated minimum temperature
    - Multiplying values by factors of 0.5x and 2x impact minimum temperature by -5ºC and +10ºC respectively
- Tower optical properties
  - Composite IR emissivity and solar absorptivity affect hot temperature results by tens of ºC per 0.1 value change

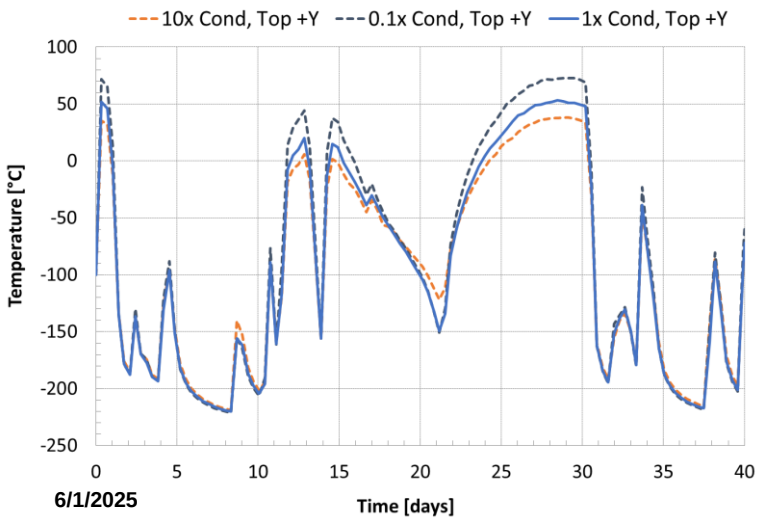

Thermal Conductivity

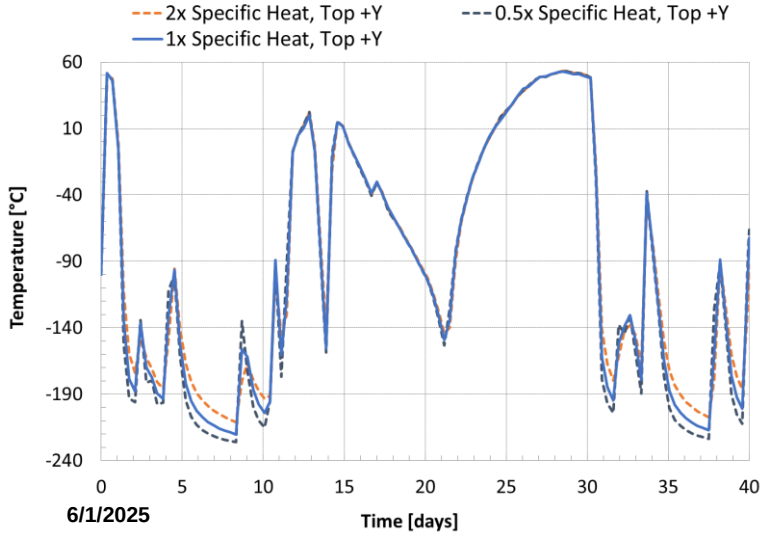

Specific Heat

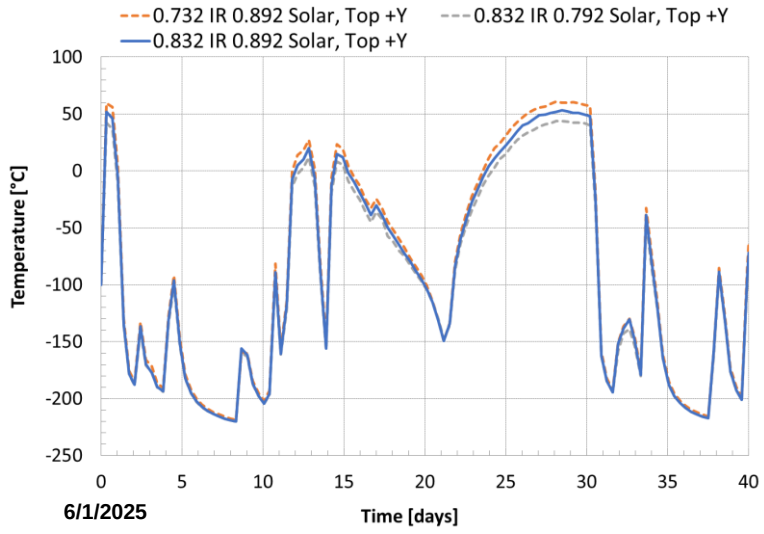

Optical Properties

Findings

Tower Operations:

- Maximum tower temperature is well below material glass transition temperature of 140ºC
- Large vertical and horizontal gradients across tower from terrain induced solar occlusion and cross member shadowing
- Maximum tower thermal induced displacement is small (0.76 cm), with highest stresses at welded interfaces
- Weld operations are impacted by minimum acceptable joint temperature at tower base with diminishing returns below -70ºC

Lunar Environment Modeling:

- Thermal results align with predicted yearly illumination percentages from previous studies
- Flat ground plane assumption is not adequate for prediction of temperature timelines
- Incident illumination and surface temperature are extremely location sensitive and precise coordinates are necessary
- Inclusion of solar diameter (subtended) angle affects thermal timeline results
- LRO seasonal average surface temperature data are not sufficient for boundary node assumption for temperature timelines

Material Property Sensitivity:

- Surface temperature differences between using DSNE and Feng 2019 optical properties negligibly affect tower temperatures
- Composite thermal conductivity significantly affects hot temperature results if changed by a factor of ≥2
- Composite specific heat affects results transition to cold and associated minimum temperature
- Composite IR emissivity and solar absorptivity can significantly affect hot temperature results if changed by ≥0.2

Future Work

Investigation of:

- Composite surface treatments to potentially minimize temperature fluctuations
- Tower being partially covered by lunar regolith dust during assembly process
- Inclusion of solar panels (static and sun tracking) and associated support equipment
- Incorporation of thermal isolation barriers at tower base to increase weld operational timespan
- Thermal gradients through structural member thickness
- Local thermal structural analysis of the joints during welding process
- Incremental build and weld configurations associated with determined assembly process and timeline
- Impacts of support platform (e.g., lander) and assembly robotics at tower base
- Alternative locations of interest across lunar south pole using improved surface mesh generation techniques

References

[1] S. Miller, “Thermoplastic Development for Exploration Applications (TDEA) Project Programmatic and Technical Overview NIAR-NASA Meeting,” 2022. Available: https://ntrs.nasa.gov/citations/20220012507

[2] M. K. Mahlin, “Tall Lunar Tower,” Nov. 02, 2022. Available: https://ntrs.nasa.gov/citations/20220016161

[3] F. B. Leahy, “SLS-SPEC-159, Cross-Program Design Specification for Natural Environments (DSNE),” Oct. 2021. Available: https://ntrs.nasa.gov/citations/20210024522

[4] B. D. Hamill, R. G. Schunk, and L. R. Erickson, “Human Landing System Lunar Thermal Analysis Guidebook,” Jan. 2021, Available: https://ntrs.nasa.gov/citations/20210010030

[5] “Lunar Reconnaissance Orbiter - NASA Science,” Available: https://science.nasa.gov/mission/lro/

[6] “Lunar Orbital Data Explorer - Data Set Browser,” ode.rsl.wustl.edu. https://ode.rsl.wustl.edu/moon/datasets

[7] J. P. Williams et al., “Seasonal Polar Temperatures on the Moon,” vol. 124, no. 10, pp. 2505–2521, Oct. 2019, doi: https://doi.org/10.1029/2019je006028.

[8] “QuickMap,” quickmap.lroc.asu.edu. Available: https://quickmap.lroc.asu.edu

[9] “Toray Cetex® TC1225 - Toray Advanced Composites,” Available: https://www.toraytac.com/product-explorer/products/gXuK/Toray-Cetex-TC1225

[10] C. Ageorges, L. Ye, Y.-W. Mai, and M. Hou, “Characteristics of resistance welding of lap shear coupons. Part I: Heat transfer,” Composites Part A: Applied Science and Manufacturing, vol. 29, no. 8, pp. 899–909, Aug. 1998, doi: https://doi.org/10.1016/S1359-835X(98)00022-0.

[11] “Horizons System,” Available: https://ssd.jpl.nasa.gov/horizons/

[12] L. Erickson, C. Gomez, B. Hamill, and G. Schunk, “Lunar Thermal Analysis Guidebook: Thermo-physical and Optical Properties of Lunar Regolith.” Available: https://ntrs.nasa.gov/api/citations/20220013412

[13] Dipl.-I. Univ, B. Philipp, and Hager, “Dynamic thermal modeling for moving objects on the Moon.” Available: https://mediatum.ub.tum.de/doc/1143820/956812.pdf

[14] P. O. Hayne et al., “Global Regolith Thermophysical Properties of the Moon From the Diviner Lunar Radiometer Experiment,” Journal of Geophysical Research: Planets, vol. 122, no. 12, pp. 2371–2400, Dec. 2017, doi: https://doi.org/10.1002/2017je005387.

[15] A. Martinez and M. A. Siegler, “A Global Thermal Conductivity Model for Lunar Regolith at Low Temperatures,” Journal of Geophysical Research: Planets, vol. 126, no. 10, Oct. 2021, doi: https://doi.org/10.1029/2021je006829.

[16] R. Woods-Robinson, M. A. Siegler, and D. A. Paige, “A Model for the Thermophysical Properties of Lunar Regolith at Low Temperatures,” Journal of Geophysical Research: Planets, vol. 124, no. 7, pp. 1989–2011, Jul. 2019, doi: https://doi.org/10.1029/2019je005955

[17] J. Feng, M. A. Siegler, P. O. Hayne, and D. T. Blewett, “Lunar Regolith Properties Constrained by LRO Diviner and Chang’e-2 Microwave Radiometer Data,” NASA ADS, p. 3176, Mar. 2019, Available: https://ui.adsabs.harvard.edu/abs/2019LPI....50.3176F/abstract

[18] J. Feng, M. A. Siegler, and P. O. Hayne, “New Constraints on Thermal and Dielectric Properties of Lunar Regolith from LRO Diviner and CE-2 Microwave Radiometer,” Journal of Geophysical Research: Planets, vol. 125, no. 1, Jan. 2020, doi: https://doi.org/10.1029/2019je006130

[19] “Lunar Thermal Analysis Guidebook, Part 3 | NESC Academy Online,” nescacademy.nasa.gov. https://nescacademy.nasa.gov/video/43723e634fe44646aef30b745640ad4d1d

[20] C. Gomez, B. Hamill, G. Schunk, and L. Erickson, “Lunar Surface 3D Terrain Modeling,” Sep. 06, 2022. Available: https://ntrs.nasa.gov/citations/20220013302

[21] “Planetary Data System,” Available: https://pds.nasa.gov/

[22] S. Bryant, “Lunar Pole Illumination and Communications Maps Computed from Goldstone Solar System Radar Elevation Data,” 2009. Available: https://ipnpr.jpl.nasa.gov/progress_report/42-176/176C.pdf

[23] E. Mazarico, G. A. Neumann, D. E. Smith, M. T. Zuber, and M. H. Torrence, “Illumination conditions of the lunar polar regions using LOLA topography,” Icarus, vol. 211, no. 2, pp. 1066–1081, Feb. 2011, doi: https://doi.org/10.1016/j.icarus.2010.10.030.

[24] D. De Rosa et al., “Characterization of Potential Landing Sites for the European Space Agency’s Lunar Lander Project,” NASA ADS, p. 1585, Mar. 2012, Available: https://ui.adsabs.harvard.edu/abs/2012LPI....43.1585D/abstract

[25] P. Gläser et al., “Illumination conditions at the lunar south pole using high resolution Digital Terrain Models from LOLA,” Icarus, vol. 243, pp. 78–90, Nov. 2014, doi: https://doi.org/10.1016/j.icarus.2014.08.013.

[26] P. Gläser, J. Oberst, G. A. Neumann, E. Mazarico, E. J. Speyerer, and M. S. Robinson, “Illumination conditions at the lunar poles: Implications for future exploration,” Planetary and Space Science, vol. 162, pp. 170–178, Nov. 2018, doi: https://doi.org/10.1016/j.pss.2017.07.006.

[27] M. Raya, Najmeh Bazmohammadi, D. Saha, J. C. Vasquez, and J. M. Guerrero, “Optimal multi-site selection for a PV-based lunar settlement based on a novel method to estimate sun illumination profiles,” Advances in space research, vol. 71, no. 5, pp. 2059–2074, Mar. 2023, doi: https://doi.org/10.1016/j.asr.2022.12.048.

[28] “Artemis Campaign Development ACD-50044 Revision A National Aeronautics and Space Administration Lunar Surface Data Book,” 2023. Available: https://ntrs.nasa.gov/api/citations/20230007818

[29] P. Gläser and D. Gläser, “Modeling near-surface temperatures of airless bodies with application to the Moon,” Astronomy & Astrophysics, vol. 627, p. A129, Jul. 2019, doi: https://doi.org/10.1051/0004-6361/201935514.

BACKUP

Tower Middle Results: 0 to 365 days

- Near continuous solar illumination at middle of tower (~85% of year)
  - Temperature variations caused mostly by cross-member shadowing (low solar elevation angle)
  - Maximum 7 days of total solar occlusion by terrain during winter season